

Cellular Long Chain Fatty Acid Uptake by CD36: Identifying an Amino Acid That Plays a  
Critical Role and Assessing Physiological Impact in Bone Marrow Derived Macrophages

by

Julia Elizabeth Piché

A thesis submitted in partial fulfillment of the requirements for the degree of

Master of Science

Medical Sciences – Oral Biology  
University of Alberta

© Julia Elizabeth Piché, 2020

## Abstract

Long chain fatty acids (LCFA) serve essential functions in human cells, and the presence of too little or too much could have detrimental effects. LCFA can enter cells through passive diffusion, also known as flip-flop, but the majority enter in association with a protein allowing regulation and unidirectional transport. Proteins associated with LCFA transport are fatty acid transport proteins and cluster of differentiation 36 (CD36). CD36 has many roles in the body, including binding thrombospondin-1 and being a macrophage scavenger receptor, but its connection with LCFA transport has only been investigated since 1981. There is controversy surrounding whether CD36 is independently transporting LCFA across the plasma membrane or involved in a signalling pathway increasing uptake. This research project aimed to identify a single amino acid mutation that does not disrupt the expression of CD36 or its ability to signal while decreasing LCFA uptake. This mutation could then be used to determine if the loss of CD36 LCFA uptake has biological effects in macrophage phenotype expression. Through two different methods, we demonstrated that the substitution of lysine 164 with glutamine (K164Q) significantly decreased LCFA uptake *in vitro* in HEK293T/17 cells. This mutant had a significant 45.7% decrease in LCFA transport compared to Wildtype CD36 and was not statistically different than cells without CD36. Using CD36-TLR2 signalling with a secretory alkaline phosphatase reporter assay dependent on NF $\kappa$ B activation, this mutation did not significantly decrease CD36's ability to signal (Wildtype CD36,  $1.679 \pm 0.163$  AU vs K164Q CD36,  $1.6436 \pm 0.102$  AU; No CD36,  $1.329 \pm 0.161$  AU). Low transfection efficiency prevented a conclusion on the impact on macrophage phenotype, but the collected data suggest this can be proven in the near future with an optimized protocol. Of the three cell types activated by IL-4 to M2 expression, Wildtype CD36 cells had the largest increase in an M2 marker, while K164Q CD36 had the smallest increase. This project encourages future work

on the topic by confirming decreased M2 expression in macrophages without LCFA uptake via CD36 and opens up the possibility of examining the exclusive loss of CD36 LCFA uptake in a mouse model allowing studies relevant to wound healing and the progression of various conditions related to LCFA transport.

## Preface

This thesis is an original work by Julia Elizabeth Piché.

All experiments performed by myself except for the collection of bone marrow, which was performed by another member of the Febbraio Lab.

No part of this thesis has been previously published.

## Acknowledgements

This thesis would not have been possible without generous funding from the Canadian Institutes of Health Research, University of Alberta Faculty of Graduate Studies and Research, University of Alberta School of Dentistry, and University of Alberta Faculty of Medicine and Dentistry. I would also like to thank the Cardiovascular Research Centre at The University of Alberta for the use of their equipment.

Thank you for the academic support from everyone in the Biomedical and Oral Maxillofacial Research Unit and the support staff in The Department of Dentistry. I would like to specifically highlight my supervisors, Dr. Maria Febbraio and Dr. Ava Chow, for all of their guidance and unwavering support throughout my program. Thank you to Dr. John Ussher for being a member of my supervisory committee. To the past and present students in the Febbraio Lab, you have my greatest appreciation for sharing this journey through graduate studies with all of its ups and downs.

Finally, thank you to my parents who pretended to be okay with me moving 1,300 km away to continue my education.

## Table of Contents

<b>List of Tables</b> .....	<b>ix</b>
<b>List of Figures</b> .....	<b>x</b>
<b>List of Abbreviations</b> .....	<b>xiii</b>
<b>Introduction</b> .....	<b>1</b>
<i>Long Chain Fatty Acids</i> .....	<i>1</i>
Overview .....	1
Transport.....	2
<i>CD36</i> .....	3
Overview .....	3
LCFA Uptake .....	4
Structure-Function Relationship.....	7
<i>Macrophage</i> .....	8
Overview .....	8
Phenotypes.....	8
Role of CD36.....	9
<i>Rationale</i> .....	10
<i>Research Question and Aims</i> .....	10
<b>Materials and Methods</b> .....	<b>11</b>
<i>Plasmid</i> .....	<i>11</i>
Wildtype .....	11
Mutant CD36 .....	12
Transformation .....	13
Plasmid Preparation.....	14
Analysis .....	14
<i>Fatty Acid Uptake Assays</i> .....	<i>15</i>

Cell Growth .....	15
Transfection .....	16
Preliminary FA Uptake Assay .....	16
Analysis .....	16
FA Uptake Assay with BODIPY FL C16 .....	17
Analysis .....	17
<i>Secretory Alkaline Phosphatase (SEAP) Assay</i> .....	17
Cell Growth .....	17
Transfection .....	18
SEAP Assay.....	18
Analysis .....	19
<i>Immunofluorescence</i> .....	19
<i>Bone Marrow Derived Macrophages (BMDM)</i> .....	19
Endotoxin-free Plasmid Preparation.....	19
Collection of Bone Marrow .....	20
Differentiation, Transfection, and Activation .....	20
Flow Cytometry .....	22
Modified Flow Cytometry .....	22
<b>Results</b> .....	<b>24</b>
<i>K164Q Significantly Decreases FA Uptake by CD36</i> .....	24
<i>K164Q does not significantly impact CD36 signaling in response to LTA</i> .....	25
<i>BMDM M2 Phenotype Expression May be Dependent on CD36 Mediated FA Uptake</i> .....	26
<i>Amxa Nucleofector System Does Not Produce a High Transfection Efficiency</i> .....	29
<b>Discussion</b> .....	<b>33</b>
<i>K164Q Significantly Decreases LCFA Uptake by CD36</i> .....	33
<i>K164Q Does Not Significantly Impact CD36 Signaling in Response to LTA</i> .....	35
<i>BMDM M2 Phenotype Expression May be Dependent on CD36 Mediated LCFA Uptake</i> .....	36

*Amxa Nucleofector System Does Not Produce High Transfection Efficiency*..... 36

*Limitations* ..... 37

*Clinical Opportunities* ..... 38

*Future Directions* ..... 38

**Conclusion** ..... 40

**References** ..... 41

## List of Tables

<b>Table 1. Primers used to create point mutations in plasmid .....</b>	<b>12</b>
<b>Table 2. PCR protocol to create point mutation in plasmid.....</b>	<b>13</b>
<b>Table 3. Primers used for Standard Sanger DNA Sequencing .....</b>	<b>15</b>
<b>Table 4. Percent decrease in FA uptake using a FA Uptake Kit. Values normalized to GFP expression and percent decrease refers to the comparison of cells expressing a mutant CD36 to cells expressing Wildtype CD36 after one hour.....</b>	<b>25</b>

## List of Figures

<b>Figure 1. Classifications of fatty acids based on hydrocarbon chain length.....</b>	<b>1</b>
<b>Figure 2. Simplified structure of CD36 highlighting the position in the plasma membrane and post translational modifications (modified from Yang 2017 <sup>16</sup>) .....</b>	<b>3</b>
<b>Figure 3. Section of CD36 from protein crystallization showing tunnels with pink palmitic acids and inset comparison of tunnel entrances with H150 in LIMP-2 undergoing conformational change to a stable F153 in CD36 (modified from Hsieh 2016 <sup>49</sup>) .....</b>	<b>8</b>
<b>Figure 4. Simplified M1/M2 macrophage phenotype scheme highlighting the main energy source and overall properties of the two extremes (modified from Fraternali 2015 <sup>56</sup>) .....</b>	<b>9</b>
<b>Figure 5. Plasmid map of mouse CD36 ORF mammalian expression plasmid, N-GFPSpark tag, created with SnapGene Viewer .....</b>	<b>11</b>
<b>Figure 6. FA Uptake Assay with BODIPY FL C16, 5-minute time point *p&lt;0.05 compared to Wildtype .....</b>	<b>25</b>
<b>Figure 7. SEAP assay using QUANTI-Blue incubated for one hour after cells in presence of LTA overnight, *p&lt;0.05 compared to K164Q .....</b>	<b>26</b>
<b>Figure 8. MFIs of BMDM in the BL1 channel of the Attune NxT Acoustic Focusing Cytometer representing GFP expression from <i>Flow Cytometry</i> protocol .....</b>	<b>27</b>
<b>Figure 9. MFIs of BMDM in the BL3 channel of the Attune NxT Acoustic Focusing Cytometer representing CD36 expression with a PerCP-Cy5.5 antibody from <i>Flow Cytometry</i> protocol ..</b>	<b>27</b>
<b>Figure 10. MFIs of BMDM in the VL1 channel of the Attune NxT Acoustic Focusing Cytometer representing F4/80 expression with a SuperBright 436 antibody from <i>Flow Cytometry</i> protocol .....</b>	<b>28</b>

Figure 12. MFIs of BMDM in the YL1 channel of the Attune NxT Acoustic Focusing Cytometer representing CD163 expression with a PE antibody from <i>Flow Cytometry</i> protocol.....	28
Figure 11. MFIs of BMDM in the RL1 channel of the Attune NxT Acoustic Focusing Cytometer representing CD38 expression with an APC antibody from <i>Flow Cytometry</i> protocol .....	28
Figure 13. MFIs of BMDM in the BL1 channel of the Attune NxT Acoustic Focusing Cytometer representing GFP expression from <i>Modified Flow Cytometry</i> protocol .....	29
Figure 16. MFIs of BMDM in the RL1 channel of the Attune NxT Acoustic Focusing Cytometer representing CD38 expression with an APC antibody from <i>Modified Flow Cytometry</i> protocol .....	30
Figure 15. MFIs of BMDM in the VL1 channel of the Attune NxT Acoustic Focusing Cytometer representing F4/80 expression with a SuperBright 436 antibody from <i>Modified Flow Cytometry</i> protocol .....	30
Figure 14. MFIs of BMDM in the BL3 channel of the Attune NxT Acoustic Focusing Cytometer representing CD36 expression with a PerCP-Cy5.5 antibody from <i>Modified Flow Cytometry</i> protocol .....	30
Figure 18. Histogram of BMDM transfected with Wildtype and activated by IL-4 in the BL1 channel of the Attune NxT Acoustic Focusing Cytometer representing GFP expression from <i>Modified Flow Cytometry</i> protocol .....	31
Figure 17. MFIs of BMDM in the YL1 channel of the Attune NxT Acoustic Focusing Cytometer representing CD163 expression with a PE antibody from <i>Modified Flow Cytometry</i> protocol.	31
Figure 20. Histogram of Untransfected BMDM activated by IL-4 in the BL1 channel of the Attune NxT Acoustic Focusing Cytometer representing GFP expression from <i>Modified Flow Cytometry</i> protocol .....	32

**Figure 19. Histogram of BMDM transfected with K164Q and activated by IL-4 in the BL1 channel of the Attune NxT Acoustic Focusing Cytometer representing GFP expression from *Modified Flow Cytometry* protocol .....32**

**Figure 21. Structural modelling of Wildtype and K164Q CD36 with fatty acid binding sites in green created with The PyMOL Molecular Graphics System, V 2.4.0 (Provided by Zahra Mantaka, unpublished) and chemical structures of lysine and glutamine .....34**

## List of Abbreviations

APC	Allophycocyanin
AMP	Adenosine monophosphate
BCECF	2,7-bis(2-carboxyethyl)-5(6)-carboxy-fluorescein
BMDM	Bone marrow derived macrophage
BODIPY	Boron dipyrromethene
BSA	Bovine serum albumin
CD36	Cluster of differentiation 36
CD38	Cluster of differentiation 38
CD163	Cluster of differentiation 163
CMV	Cytomegalovirus
CO <sub>2</sub>	Carbon dioxide
°C	Degrees Celsius
DAMP	Damage associated molecular pattern
DIDS	4,4'-diisothiocyanostilbene-2,2'-disulfonate
DMEM	Dulbecco's Modified Eagle Medium
DMSO	Dimethyl sulfoxide
DNA	Deoxyribonucleic acid
dNTP	Deoxyribonucleotide triphosphate
F153A	Phenylalanine replaced by alanine at site 153 in CD36 protein
F153N	Phenylalanine replaced by asparagine at site 153 in CD36 protein

F153W	Phenylalanine replaced by tryptophan at site 153 in CD36 protein
FA	Fatty acid
FAT	Fatty acid translocase
FATP	Fatty acid transport protein
FBS	Fetal bovine serum
FPE	N- (fluorescein-5-thiocarbamoyl)-1,2-dihexadecanoyl-sn-glycero-3- phosphoethanolamine
GFP	Green fluorescent protein
HBSS	Hank's Balanced Salt Solution
IL-4	Interleukin-4
IMDM	Iscoe's Modified Dulbecco Medium
K164R	Lysine replaced by arginine at site 164 in CD36 protein
K164Q	Lysine replaced by glutamine at site 164 in CD36 protein
K164Y	Lysine replaced by tyrosine at site 164 in CD36 protein
LB	Luria-Bertani
LCCM	L929 containing culture medium
LCFA	Long chain fatty acid
LDL	Low density lipoprotein
LIMP	Lysosomal integral membrane protein
LPS	Lipopolysaccharide
LTA	Lipoteichoic acid
M-FABP	Muscle fatty acid binding protein

MCFA	Medium chain fatty acid
MFI	Mean fluorescence intensity
min	Minute
ml	Millilitre
mM	Millimolar
NF- $\kappa$ B	Nuclear factor kappa light chain enhancer of activated B cells
ng	Nanogram
OD	Optical density
ORF	Open reading frame
PBS	Phosphate buffered saline
PCR	Polymerase chain reaction
PE	Phycoerythrin
PerCP-Cy5.5	Peridinin chlorophyll protein – cyanine 5.5
RFU	Relative fluorescent units
RNA	Ribonucleic acid
RPM	Revolutions per minute
RPMI	Roswell Park Memorial Institute 1640 medium
SCFA	Short chain fatty acid
SEAP	Secretory Alkaline Phosphatase
sec	Second
SITS	4-acetamido-4'-isothiocyanostilbene-2,2'-disulfonic acid
SLC27	Solute carrier family 27

---

SOC	Super optimal broth with catabolite repression
SRB	Scavenger receptor B
TE	Trisaminomethane ethylenediaminetetraacetic acid
TLR2	Toll like receptor 2
U	Unit
μg	Microgram
μl	Microliter
VLCFA	Very long chain fatty acid
xg	Relative centrifugal force

---

## Introduction

### Long Chain Fatty Acids

#### Overview

Fatty acids (FA), comprised of a hydrocarbon chain bonded to carboxylic acid, can be grouped by the length of their hydrocarbon chain (Figure 1). Short chain fatty acids (SCFA) have 1-6 carbons, medium chain fatty acids (MCFA) have 7-12 carbons <sup>1</sup>, long chain fatty acids (LCFA) have 13-20 carbons, and very long chain fatty acids (VLCFA) have greater than 20 carbons <sup>2</sup>. LCFA, including palmitic acid and oleic acid, compose the majority of FA in mammalian cells <sup>2</sup>.

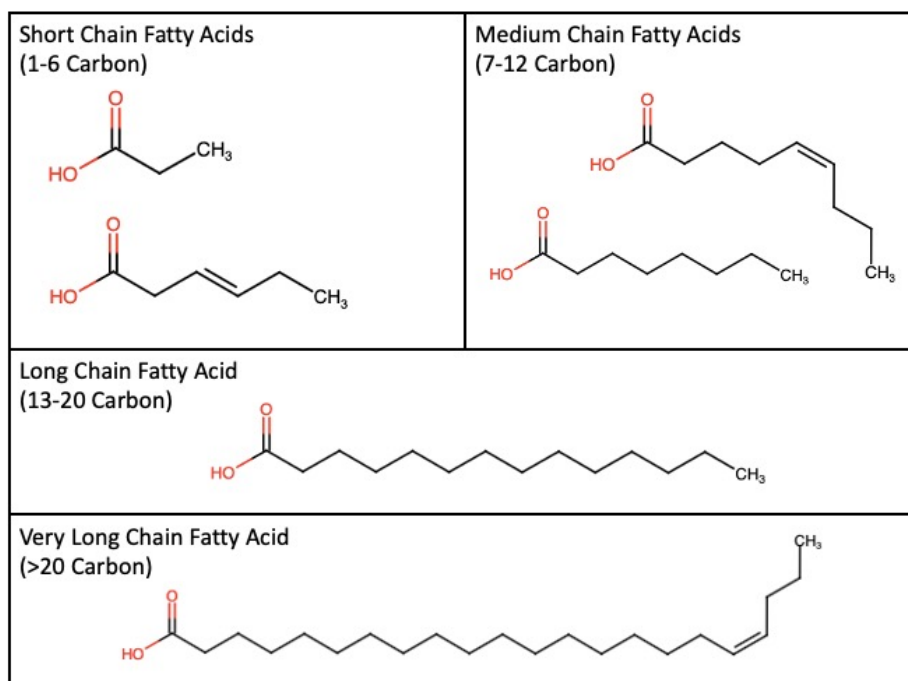


Figure 1. Classifications of fatty acids based on hydrocarbon chain length

Palmitic acid, the most abundant saturated FA found in humans, has 16 carbons with no double bonds (a saturated FA). It can be sourced through the diet in palm oil, meat, and dairy products as well as synthesized in the body <sup>3</sup>. Palmitic acid is the most abundant FA found in phospholipids, which compose the cell membrane, and triacylglycerols, which are the main form of FA storage <sup>3</sup>. An imbalance of palmitic acid in the body has been linked to atherosclerosis, tumour growth, metabolic disorders, cancer, neurodegenerative diseases, and non-alcoholic fatty

liver disease<sup>3</sup>. Oleic acid is the most abundant monounsaturated FA in the diet, found in high concentrations in dietary oils<sup>4</sup>. A diet high in oleic acid has been associated with satiation, decreased obesity, and therefore decreased risks of developing obesity associated conditions, including metabolic syndrome<sup>5</sup>. Due to LCFA levels being associated with a wide variety of pathological conditions, understanding how they are regulated for uptake and metabolism in the human body is extremely important.

### Transport

LCFA are capable of entering the cell through passive diffusion (also known as flip-flop), but this mechanism does not allow regulation of this metabolically important energy source<sup>6</sup>.

Protein transport of LCFA allows targeted uptake from the bloodstream, even in times of low circulating levels, and immediate modifications by associated proteins upon entering the cells, thus creating a concentration gradient and preventing them from leaving the cell<sup>6</sup>. Proteins that have been proposed to be involved in the transport of LCFA include members of the fatty acid transport protein family (FATP) and cluster of differentiation 36 (CD36).

The first FATP member was identified from a cDNA library from 3T3-L1 adipocytes (a murine cell line used extensively to mimic fat cells from white adipose tissue) in 1994<sup>7</sup>. That protein is currently known as FATP1, the founding member of a family of 6 isoforms, FATP1-6<sup>6</sup>, also known as solute carrier family 27 (SLC27) A1-6<sup>8</sup>. The isoforms have distinct expression levels across tissues; for example, FATP5 is exclusively found in the liver and FATP6 in the heart<sup>8</sup>. All family members possess a conserved FATP sequence of 311 amino acids and an adenosine monophosphate (AMP) binding domain while ranging between 63 and 80 kDa in size<sup>8</sup>.

Although it is widely accepted that FATP are involved in LCFA transport through a variety of *in vivo* and *in vitro* experiments, the exact mechanism of uptake is unknown. The other protein involved in LCFA transport, and of more importance to this project, is CD36.

## CD36

### Overview

CD36 (Figure 2), previously known as fatty acid translocase (FAT), scavenger receptor class B (SRB) member 2, thrombospondin receptor, and platelet glycoprotein IIIb<sup>9</sup>, is an 88kDa transmembrane protein<sup>10</sup> which was first reported as platelet glycoprotein IV in 1977<sup>11</sup>. In 2017, a scavenger receptor nomenclature consensus panel was convened by the US National Institutes of Health, and suggested scavenger receptor class B member 2 for the official name of CD36; adherence to this nomenclature system is sporadic<sup>12</sup>. The CD36 gene is conserved across many species, including human, chimpanzee, mouse, zebrafish, drosophila, and roundworm<sup>9</sup>. CD36 is found in most tissues throughout the body but has relatively high expression in adipose, heart, and spleen, as determined through ribonucleic acid (RNA)-sequencing<sup>13</sup>. Another RNA-sequencing publication which didn't analyze adipose tissue, but included skeletal muscle, reported high expression in heart, skeletal muscle, and spleen<sup>14</sup>. High expression correlates with tissues involved in the storage and metabolism of LCFA (adipose, heart, skeletal muscle) and clearance of apoptotic cells (spleen)<sup>15</sup>.

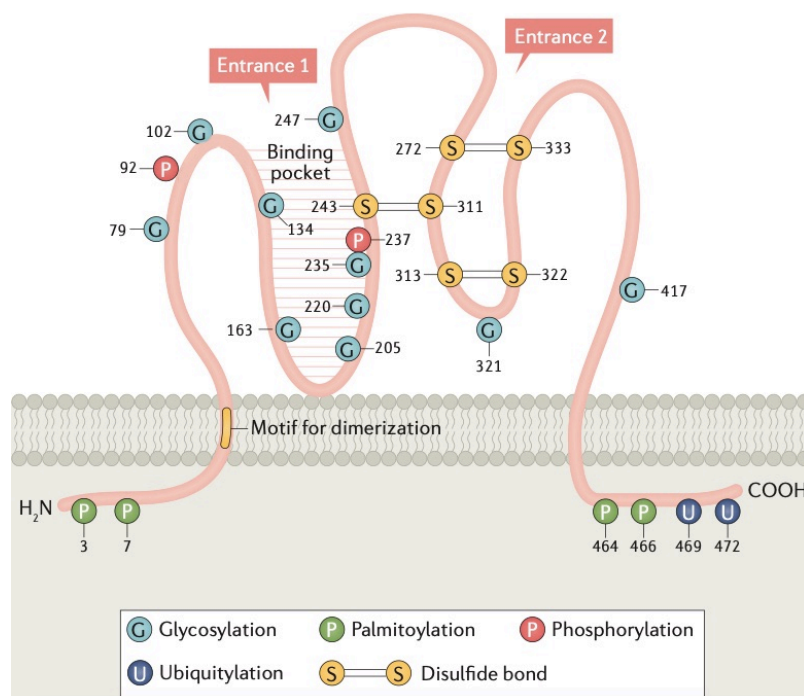


Figure 2. Simplified structure of CD36 highlighting the position in the plasma membrane and post translational modifications (modified from Yang 2017<sup>16</sup>)

CD36 interacts with several ligands, including the matricellular protein thrombospondin-1<sup>17</sup>, which leads to a variety of downstream events. CD36 binding to thrombospondin-1<sup>17</sup> leads to a signalling cascade that culminates in endothelial cell apoptosis, ultimately inhibiting angiogenesis<sup>18</sup>. CD36 is therefore involved in the regulation of conditions that involve generation of new vasculature, including inflammation, new growth of tumours, tissue growth, and repair<sup>19</sup>. The most ancient role of CD36 is considered to be as a scavenger receptor for apoptotic cells. In *Drosophila*, CD36 is known as Croquemort and fulfills this ancient function<sup>20</sup>. Accumulation of apoptotic cells can lead to alterations in differentiation during embryogenesis<sup>20</sup> and to autoimmune disease<sup>21</sup>. As a scavenger receptor, CD36 recognizes alterations in FA and phospholipids expressed on lipoproteins and cell membranes, so called damage associated molecular patterns (DAMPs)<sup>22</sup>. CD36 expressed on macrophages contributes to atherosclerosis by forming foam cells through recognition and internalization of oxidized low density lipoproteins (LDL)<sup>23</sup>. CD36 expressed in microglial cells may play a role in Alzheimer's disease by recognizing and internalizing  $\beta$ -amyloid, ultimately triggering neurodegeneration<sup>24</sup>. Endothelial CD36 serves as a binding site for red blood cells infected with the malaria parasite, allowing progression of the disease<sup>25</sup>. Depending on the ligand, signaling pathways downstream of CD36 can have a variety of outcomes and other membrane receptors are usually involved in this process. For example, CD36 has been shown to interact with toll like receptors<sup>26,27</sup>, tetraspanins, and integrins<sup>28</sup>. CD36 is also involved in LCFA uptake, the major focus of this thesis.

### LCFA Uptake

In 1981, researchers reported that the passage of LCFA into rat adipocytes was protein mediated with limited unfacilitated passage through the cell membrane<sup>29</sup>. This was discovered by isolating rat adipocytes, introducing radioactively labelled oleate, and monitoring the rate of uptake. The rate of uptake remained the same, even when glucose was present, which resulted in increased FA esterification in the cell. This suggested the uptake was independent of FA metabolism. The uptake was inhibited by the introduction of phloretin, a common inhibitor of membrane transport processes, resembled protein kinetics transport at low and physiological concentrations, and diffusion kinetics at high concentrations. Further work with kinetic analyses supported the presence of protein transport<sup>30</sup> specific for FA with a free carboxylic acid and a hydrocarbon chain of at least 9 carbon atoms. Uptake was irreversibly inhibited by 4,4'-

diisothiocyanostilbene-2,2'-disulfonate (DIDS) and 4-acetamido-4'-isothiocyanostilbene-2,2'-disulfonic acid (SITS). Utilizing the irreversible binding of DIDS to the protein, electrophoresis was performed to determine the protein was approximately 85 kDa<sup>30</sup>. The protein was named FAT and later found to be homologous with human CD36 (85% similarity). This was accomplished by isolating the cDNA from a rat adipocyte library, determining the amino acid sequence, and searching a database for related sequences<sup>10</sup>.

The first evidence of reversible LCFA binding to CD36 was reported in 1996<sup>31</sup>. CD36 was purified from rat adipocytes and incubated in solution with radioactive FA. The unbound FA was removed from solution with a Lipidex assay before determining the moles of bound FA for every mole of CD36. CD36 was found to have a high affinity reversible binding for a variety of LCFA, thus eliminating the idea that the binding is due to covalent palmitoylation. Through homology with human muscle fatty acid binding protein (M-FABP), it was also predicted that the binding site on CD36 for LCFA falls between residues 127 and 279. More specifically, the residues 139 to 154, which were predicted to be alpha-helical, would be hydrophobic. The hydrophobicity of this region suggested it would lie within the plasma membrane and could serve as a LCFA entrance.

The creation of a CD36 null mouse model through homologous recombination<sup>32</sup> started to reveal the systemic impact of LCFA uptake by CD36. The loss of CD36 resulted in a significant reduction of surface-bound oxidized LDL on peritoneal macrophages<sup>32</sup>. In the absence of CD36, fasted mice had increased free FA and triacylglycerol in plasma, decreased FA transport in adipocytes, and decreased plasma glucose levels<sup>32</sup>. On the other end of the spectrum, overexpression of CD36 in mouse muscle resulted in increased blood glucose levels, lower triglycerides, and lower FA<sup>33</sup>. Further work with CD36 null mice confirmed the uptake of iodinated LCFA analogs were decreased in heart, skeletal muscle, and adipose tissue. Palmitate was less incorporated into triglycerides, but increased in diglycerides in adipose tissue<sup>34</sup>. Looking specifically at the intestine to determine if CD36 was involved in the uptake of dietary FA, it was found that without CD36, there is LCFA accumulation in the small intestine due to a decrease in secreted lipoproteins<sup>35</sup>.

There has been considerable debate over the need for protein-mediated FA transport because free FA are able to cross the membrane alone and the mechanism of protein transport has yet to be

unequivocally proven<sup>36</sup>. One approach to address this controversy was creating a protocol that allows the separate analysis of LCFA uptake and metabolism. With the use of pH sensitive fluorescent indicators 2,7-bis(2-carboxyethyl)-5(6)-carboxy-fluorescein (BCECF) or N-(fluorescein-5-thiocarbamoyl)-1,2-dihexadecanoyl-sn-glycero-3-phosphoethanolamine (FPE) in the cell, binding of oleic acid produced a decrease in FPE fluorescence and transport produced a decrease in BCECF fluorescence<sup>37</sup>. The rate of transport of oleic acid in cells was the same whether CD36 was present or not, but binding and the amount of oleic acid in the cell was increased over time in cells expressing CD36. The rate of transport remained the same whether CD36 is present or not due to flip flop being a fast process, while protein transport is a relatively slow process. FA esterification was also quantified using a radioactive labelled oleic acid. Cells not expressing CD36 had higher proportions of free FA, while cells expressing CD36 had higher proportions of FA incorporated into triacylglycerols and monoglycerols<sup>37</sup>. Xu et al. concluded that CD36 promotes an increase in esterification, possibly through signalling or interactions with enzymes, which is causing the overall increase in uptake. Without CD36 present, oleic acid is capable of flip flopping within the plasma membrane, but not readily leaving the inner membrane to enter the cell.

A small portion of the human population is CD36 deficient. In a population of African-American subjects with a variety of single nucleotide polymorphisms in the CD36 gene that reduce expression, it was found that those heterozygous for the polymorphism and therefore expressing low levels of CD36, were protected from developing metabolic syndrome<sup>38</sup>. Metabolic syndrome puts individuals at higher risk of developing cardiovascular disease and type 2 diabetes and is characterized by obesity, dyslipidemia, and insulin resistance<sup>38</sup>. Those homozygous (no CD36 expression) had opposite effects, with increased triglycerides and decreased high density lipoproteins<sup>38-40</sup>. CD36 expression was not confirmed across all tissues and there is no evidence to support that expression levels are predictable from polymorphisms or expression in other tissues. There is also evidence that CD36 deficiency is a contributing factor to sudden infant death syndrome due to the inability to uptake LCFA by tissues when circulating levels are low from fasting and therefore cannot fuel thermogenesis<sup>41</sup>. The evidence supports a strong correlation between CD36 expression and LCFA uptake; however, there is still controversy as to whether CD36 is a LCFA transport protein or if it is involved in a signalling pathway that increases uptake through other means<sup>36</sup>.

### Structure-Function Relationship

CD36 contains two transmembrane domains on either side of a highly glycosylated extracellular domain <sup>42</sup> containing three disulfide bridges <sup>43</sup> (Figure 2). The extracellular domain also contains at least two distinct binding domains for thrombospondin and oxidized LDL <sup>43</sup>. The protein has two intracellular termini containing palmitoylation sites <sup>43</sup>, with a signal peptide on the amino-terminus <sup>44</sup>. These basic features of CD36 were compiled over the years by analyzing the gene and amino acid sequence but in absence of the structural data.

Determining the exact structure of a protein's crystal structure through x-ray crystallography is a complex process that is not always possible <sup>45</sup>. In the absence of x-ray crystallography, assumptions about the structure can be made based on the amino acid sequence or more accurately, comparing it with a known structure with a similar sequence <sup>46</sup>. Lysosomal integral membrane protein (LIMP)-2 is a member of the CD36 superfamily, along with SR-B1 <sup>47</sup>. All members of the family are scavenger receptors involved in innate immunity and lipid metabolism <sup>47</sup>. LIMP-2 is expressed on endosomes and lysosomes as a receptor for enteroviruses and the lysosomal protein, glucocerebrosidase, which it transports from the endoplasmic reticulum to lysosomes <sup>48</sup>. The first full structure of CD36 deduced by homology was reported in 2013. It was based on the crystal structure of LIMP-2 as reference <sup>47</sup>. LIMP-2 was found to have a channel running the length of the protein and it was predicted that CD36 shared this transmembrane channel, allowing the transfer of lipids <sup>47</sup>.

The structure of CD36 itself was determined through protein crystallization in 2016. A transmembrane channel was confirmed; however, the channel in CD36 contains two extracellular entrances <sup>49</sup> (Figure 3). Different from the homology structure is the replacement of H150 on LIMP-2, which undergoes a pH dependent conformational change, with F153, allowing one of the extracellular channel entrances in CD36 to remain open independent of its surrounding pH and thus always prepared to bind FA <sup>49</sup>. Residing close to F153 is K164, which was noted as a residue of interest at the opening of the channel <sup>49</sup>. Palmitic acid was modelled into the channel of CD36 and a close fit was found. The modelling provides strong evidence that LCFAs are able to travel through the channel, with the hydrocarbon chain entering first <sup>49</sup>.

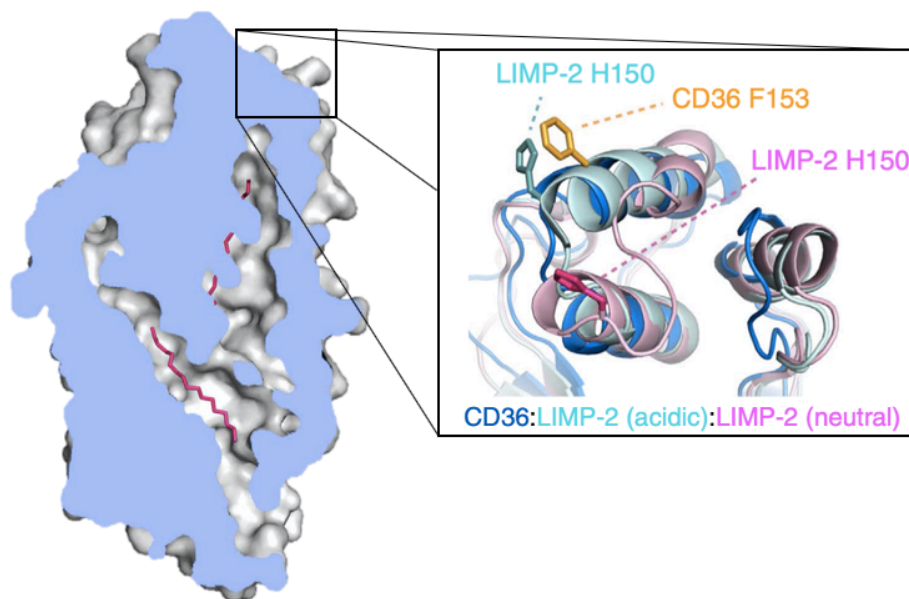


Figure 3. Section of CD36 from protein crystallization showing tunnels with pink palmitic acids and inset comparison of tunnel entrances with H150 in LIMP-2 undergoing conformational change to a stable F153 in CD36 (modified from Hsieh 2016<sup>49</sup>)

## Macrophage

### Overview

Macrophages are key players in the immune system found in all mammalian tissues<sup>50</sup> and classified as phagocytes with the ability to recognize and engulf foreign bodies<sup>51</sup>. They help control homeostasis and react to changes in their environment, sometimes with detrimental effects<sup>50</sup>. Pathologically they contribute to cancer, fibrosis, atherosclerosis, neurodegeneration, and osteoporosis<sup>50</sup>. Tissue resident macrophage derive from the yolk sac *in utero* and are the first source of macrophages for our tissues; they self-renew into and throughout adulthood<sup>51</sup>. Throughout life, macrophages can be produced through hematopoiesis, the process of hematopoietic stem cells in bone marrow differentiating into various cell types, including circulating monocytes, and ultimately becoming macrophages<sup>51</sup>.

### Phenotypes

Macrophages can present in various phenotypic forms depending on their environment and functions that need to be performed. At least nine different groupings based on source, activation, and markers have been described<sup>51</sup>. There are multiple different identification

schemes to describe these phenotypes; the M1/M2 scheme is one of the best known. A high-level of understanding can be explained on a spectrum with M1 and M2 as the two extremes <sup>52</sup> (Figure 4). Macrophage populations can be characterized by differences in markers, cytokines, and functions <sup>53</sup>. M1 populations, also referred to as classically activated, identify as pro-inflammatory and use glucose as their main energy source <sup>54</sup>. They are associated primarily with an antimicrobial response <sup>55</sup>. M2 populations, also referred to as alternatively activated, identify as anti-inflammatory in nature and use LCFA as their main energy source <sup>54</sup>. They are primarily associated with wound healing <sup>55</sup>.

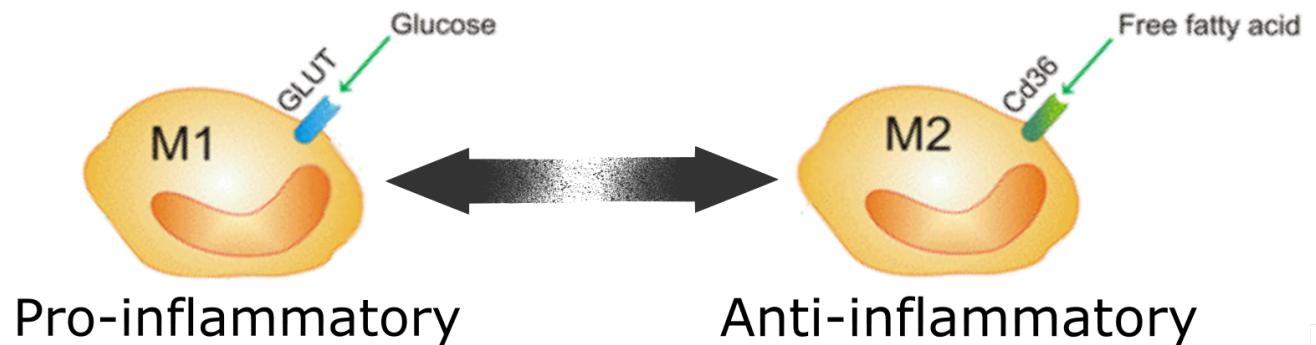


Figure 4. Simplified M1/M2 macrophage phenotype scheme highlighting the main energy source and overall properties of the two extremes (modified from Fraternali 2015 <sup>56</sup>)

### Role of CD36

As previously mentioned, M2, or alternatively activated macrophage, utilize LCFA as their main energy source. CD36 is highly expressed in this phenotype <sup>57-59</sup> in order to facilitate large amounts of LCFA uptake, making it a reliable marker for the M2 phenotype <sup>56, 60</sup>. However, there is currently no published evidence demonstrating that transport of LCFA by CD36 in macrophage (or other cell types), is independent from its signalling capabilities, and essential for the M2 phenotype. The question as to whether lack of CD36-mediated LCFA uptake in macrophages, independent of other CD36 functions, prevents them from performing downstream processes known to be characteristic of an M2 population like wound healing remains untested.

## Rationale

Despite the strong correlation between CD36 expression and LCFA uptake in cells, controversy remains as to whether the relationship exists because CD36 is transporting LCFAs across the cell membrane, if it signals to boost cellular metabolism, or a combination of these. The creation of a CD36 protein that has unaffected signalling capabilities but a reduced or inability to transport LCFA due to a mutation in the putative FA transporting channel could provide insight.

Phenylalanine 153 (F153) and lysine 164 (K164), are promising sites for this mutation as suggested by previous literature<sup>49</sup>. This mutant will be used in studies address directly whether CD36 transports LCFA across the cell membrane, or instead signals and in some way alters LCFA uptake. The identification of a specific amino acid that plays a critical role in the transport would also provide a target for designing pharmaceuticals to decrease LCFA uptake into cells. The creation of this mutant would provide a unique opportunity to study the loss of CD36 LCFA independent of its other functions, in many systems, including macrophage phenotype.

## Research Question and Aims

The research questions of this project are, 'can a single point mutation in CD36 exclusively decrease LCFA uptake and will the loss of that function skew macrophages to an M1 phenotype?'. We hypothesize that CD36 can transport LCFA across the cell membrane independently. Based on the crystal structure, we hypothesize that a single point mutation at the channel entrance will result in loss of LCFA uptake while preserving other CD36 functions. M2 macrophages depend on high energy LCFA transported by CD36 to carry out cellular CD36 functions and will therefore be skewed to an M1 phenotype. The goal of this research project is to identify an amino acid that plays a critical role in CD36-mediated cellular LCFA uptake by mutating it so that CD36 exclusively loses its ability to transport LCFA and then assess the impact of this mutation on macrophage phenotypes. The aims of this research project are:

1. Identify a single amino acid mutation that does not disrupt the expression of CD36, decreases LCFA uptake, and does not disrupt CD36 signalling.
2. Determine if the exclusive loss of LCFA transport by CD36 has biological effects in terms of macrophage phenotype.

## Materials and Methods

### Plasmid

#### Wildtype

The plasmid ‘mouse CD36 open reading frame (ORF) mammalian expression plasmid, N-green fluorescent protein (GFP) Spark tag’ was purchased from Sino Biological Inc. (catalog number: MG50422-ANG) as a lyophilized plasmid. The plasmid features a cytomegalovirus (CMV) promoter, kanamycin and hygromycin resistance genes, and GFPSpark as a fluorescent protein tag, as shown in Figure 5.

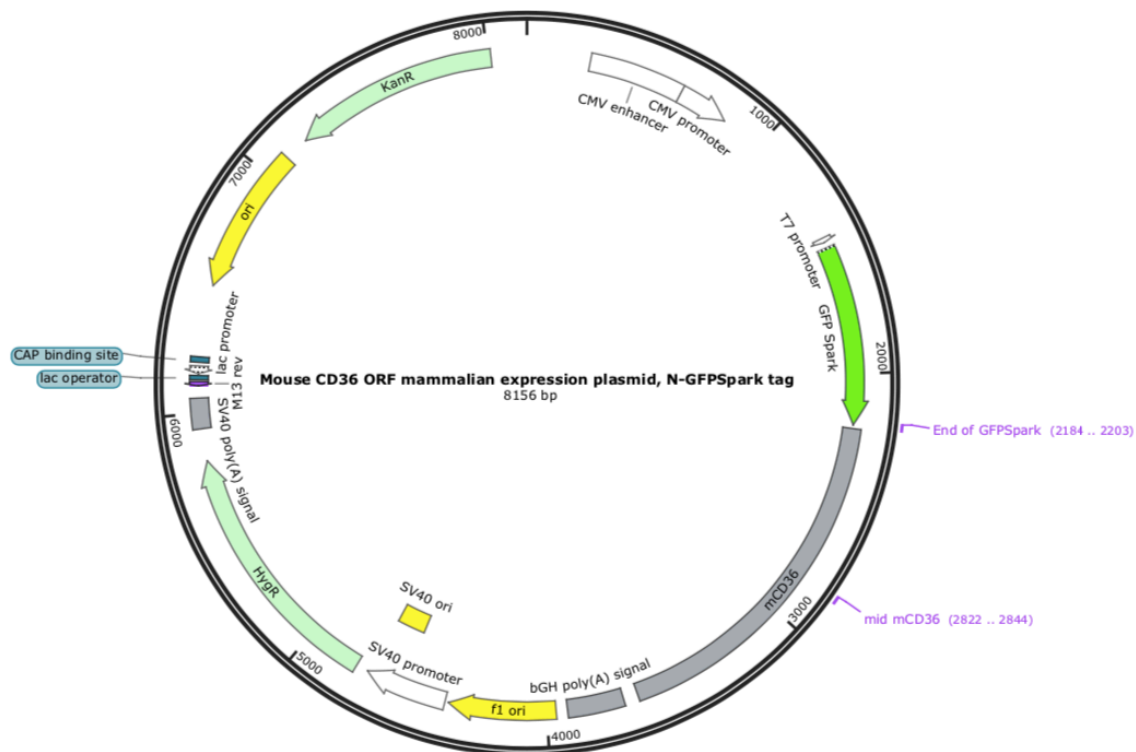


Figure 5. Plasmid map of mouse CD36 ORF mammalian expression plasmid, N-GFPSpark tag, created with SnapGene Viewer

The lyophilized plasmid was centrifuged in a microfuge for 1 minute, resuspended in 100  $\mu$ l sterile water, and incubated at room temperature for 10 minutes. The resuspended plasmid was microfuged for 10 seconds, used in *Transformation*, and the remaining was stored at  $-20^{\circ}\text{C}$ .

## Mutant CD36

Mutants were created with the Thermo Phusion Site Directed Mutagenesis Kit (catalog number F-541) with the primers, as indicated in Table 1.

Table 1. Primers used to create point mutations in plasmid
--

<i>F153A</i>
Forward – /5Phos/CTACCAAATTCAGCTGTTCAAGTTGTG
Reverse – /5Phos/ATATGTGGTGCAGCTGCTACAGC
<i>F153N</i>
Forward – /5Phos/CTACCAAATTCAAATGTTCAAGTTGTG
Reverse – /5Phos/ATATGTGGTGCAGCTGCTACAGC
<i>F153W</i>
Forward – /5Phos/CTACCAAATTCATGGGTTCAAGTTGTG
Reverse – /5Phos/ATATGTGGTGCAGCTGCTACAGC
<i>K164R</i>
Forward – /5Phos/AACTCTCTTATAAAAAGGTCCAAGTCTTCT
Reverse – /5Phos/GAGCACAACCTGAACAAATGAATT
<i>K164Q</i>
Forward – /5Phos/AACTCTCTTATAAACAGTCCAAGTCTTCT
Reverse – /5Phos/GAGCACAACCTGAACAAATGAATT
<i>K164Y</i>
Forward – /5Phos/AACTCTCTTATAAAATACTCCAAGTCTTCT
Reverse – /5Phos/GAGCACAACCTGAACAAATGAATT

A polymerase chain reaction (PCR) was set up as follows: 5  $\mu$ l of 5X Phusion HF Buffer, 0.5  $\mu$ l 10mM deoxynucleoside triphosphates (dNTPs), 0.5  $\mu$ M forward primer, 0.5  $\mu$ M reverse primer, 0.05 ng Wildtype plasmid (template deoxyribonucleic acid (DNA)), 0.25  $\mu$ l Phusion Hot Start DNA Polymerase (2U/ $\mu$ l) and sterile water to make a final volume of 25  $\mu$ l, were added together at room temperature. The protocol for the PCR is shown in Table 2 using a T100 Thermal Cycler (Bio-Rad) (catalog number 1861096).

Table 2. PCR protocol to create point mutation in plasmid			
---	--	--	--

Initial	98°C	30 sec	
Denaturation			
Denaturation	98°C	10 sec	
Annealing	62°C	30 sec	25 cycles
Extension	72°C	3 min	
Final Extension	72°C	5 min	
Hold	4°C	$\infty$	

The PCR product was subjected to gel electrophoresis to confirm amplification of the correct size plasmid before being ligated. Ligation was performed by combining 2  $\mu$ l of the PCR product, 1  $\mu$ l of 5X Rapid Ligation Buffer, 2  $\mu$ l sterile water, and 0.25  $\mu$ l T4 DNA ligase at room temperature in a microcentrifuge tube and incubating for 5 minutes before placing on ice. The ligated plasmid was then used in *Transformation*.

#### Transformation

Subcloning Efficiency DH5 $\alpha$  Competent Cells from Invitrogen (catalog number 18265-017) (previously aliquoted and stored at -80°C) were used for transformation. One aliquot of DH5 $\alpha$  cells were thawed in an ice bath, mixed with a pipette tip, and 50  $\mu$ l transferred to a pre-chilled 1.5 ml microcentrifuge tube in an ice bath. 1  $\mu$ l of resuspended plasmid was added to the cells and mixed with a pipette tip. This mixture was incubated in an ice bath. After thirty minutes, the tube was placed in a 42°C water bath for thirty seconds (heat shock) and returned to the ice bath for 2 minutes. The cells were added to 950  $\mu$ l of pre-warmed super optimal broth with catabolite

repression (SOC) medium in a culture test tube and incubated at 37°C with shaking at 250 rpm for 1 hour. The culture (50 µl or 150 µl) was plated on Luria-Bertam (LB) agar plates supplemented with kanamycin and incubated at 37°C overnight. The remaining culture was stored at 4°C in case of no growth. Single colonies that grew on the plates were used in *Plasmid Preparation* the following morning.

#### Plasmid Preparation

One colony from an overnight agar plate was transferred to 4 ml LB broth supplemented with kanamycin and incubated overnight at 37°C with shaking at 250 rpm. The plates were then stored at 4°C. A freeze down of the cells was made by combining 950 µl of culture with 50 µl of sterile glycerol and stored at -80°C. 3 ml of culture were centrifuged at 6000xg for 15 minutes at 4°C in a 5 ml centrifuge tube. The following protocol was performed with a QIAGEN Plasmid Mini Kit (catalog number 12125). The bacterial pellet was resuspended in 300 µl of Buffer P1 supplemented with Rnase A solution and LyseBlue reagent. 300 µl of Buffer P2 were added and the solution mixed by inverting the tube multiple times before incubating at room temperature for 5 minutes. 300 µl of pre-chilled Buffer P3 were added, mixed in by inverting the tube multiple times, and incubated in an ice bath for 5 minutes. This solution was centrifuged at 17,000xg for 10 minutes. The supernatant was transferred to a QIAGEN-tip 20 that was equilibrated with 1 ml Buffer QBT. After the supernatant ran through the resin, it was washed twice with 2 ml Buffer QC. The plasmid was eluted off the resin with 800 µl of Buffer QF and collected into a 2 ml microcentrifuge tube. The plasmid was precipitated with the addition of 560 µl isopropanol and centrifuged at 17,000xg for 30 minutes. The supernatant was removed, and the pellet washed with 1 ml 70% ethanol before being centrifuged at 15,000xg for 10 minutes. The supernatant was removed, the pellet was left at room temperature to dry for 10 minutes and then resuspended in 100 µl sterile water. Resuspended plasmids were used in *Analysis*, *Transfection*, and the remaining were aliquoted and stored at -20°C.

#### Analysis

All plasmid suspensions were analyzed for concentration and purity with a ThermoScientific NanoDrop 2000c Spectrophotometer (catalog number ND-2000C). Plasmid suspensions were also analyzed by gel electrophoresis to confirm concentration, purity, and correct size. The

sequence of the Wildtype plasmid was confirmed by standard Sanger DNA sequencing performed by the Molecular Biology Facility at The University of Alberta with the primers shown in Table 3.

Table 3. Primers used for Standard Sanger DNA Sequencing

*T7* – TAATACGACTCACTATAGGG

*End of GFP Spark* – GCATGGACGAGCTGTACAAG

*Mid mCD36* – CCTTACAATGACACTGTAGATGG

The locations of these primers are shown in the plasmid map in Figure 1. The sequences of the mutant plasmids were also confirmed by standard Sanger DNA sequencing by the Molecular Biology Facility at The University of Alberta with *End of GFP Spark* (Table 3) primer, which is upstream of the mutation sites.

## Fatty Acid Uptake Assays

### Cell Growth

All procedures were carried out in a level 2 biosafety cabinet with sterile materials. HEK293T/17 cells were purchased from American Type Culture Collection (ATCC) (catalog number ATCC CRL-11268). The cells were grown in Dulbecco's Modified Eagle Medium (DMEM) High Glucose (HyClone) (catalog number SH30022.01) supplemented with 10% heat inactivated fetal bovine serum (FBS), 100 U/ml penicillin, and 100 µg/ml streptomycin on tissue culture plates in a 37°C incubator with 5% CO<sub>2</sub>. When cells reached 80-90% confluency, they were split to prevent overgrowth. The medium was discarded, cells resuspended in fresh medium, and transferred to a fifteen ml centrifuge tube. The plate was rinsed with fresh medium, and this was also transferred to the previous centrifuge tube. The suspended cells were centrifuged at 300xg for 3 minutes. The supernatant was discarded, and the pellet resuspended in 2 ml of fresh medium. When carrying the cells in the same plate size, 500 µl of cells were added to fresh medium such that they were plated at approximately 25% confluency. In some cases, the remaining cells were frozen with the addition of dimethyl sulfoxide (DMSO) in a cryogenic tube and stored at -80°C.

### Transfection

HEK 293T/17 cells were plated at 25% confluency in wells of a 24 well tissue culture plate. When cells were 50-60% confluent, they were transfected with plasmids using Lipofectamine 3000 Reagent (ThermoFisher Scientific catalog number L3000001). In one microfuge tube, 25  $\mu$ l of DMEM High Glucose and 0.75  $\mu$ l Lipofectamine 3000 Reagent were mixed. In another microfuge tube, 25  $\mu$ l of DMEM High Glucose, 0.5  $\mu$ g of resuspended plasmid from *Plasmid Preparation*, and 1  $\mu$ l of P3000 Reagent were mixed. The contents of the two microfuge tubes were combined and incubated for 15 minutes at room temperature. The solution was then added dropwise into the 24 well tissue culture plate and incubated for 2 days at 37°C and 5% CO<sub>2</sub>. After 2 days, the cells were then treated as described in *Cell Growth*, except the medium was supplemented with 200  $\mu$ g/ml Hygromycin B (Invitrogen) (catalog number 10687010) for 1 week and 100  $\mu$ g/ml from that point forward.

### Preliminary FA Uptake Assay

HEK 293T/17 cells were plated in a 96 well tissue culture plate with six wells per cell type (Untransfected parental cells, Wildtype CD36, F153N, F153W, F153A, K164R, K164Q, and K164Y) and grown to an average 80-90% confluency. The preliminary FA uptake assay was performed with a Fatty Acid Uptake Kit (Sigma-Aldrich) (catalog number MAK156). The positive buffer was prepared by combining 3 ml of Assay Buffer and 6 $\mu$ l of TF2-C12 Fatty Acid Stock Solution. The negative buffer was the Assay Buffer alone. The medium was replaced with 100  $\mu$ l of DMEM High Glucose for 20 minutes to serum starve the cells. The medium was then replaced with the positive or negative buffer, three wells per type, and incubated for 1 hour. Fluorescent endpoint readings were then taken on a Synergy H1 Hybrid Multi-Mode Reader (BioTek) with bottom optics, auto scale gain, excitation at 485 nm, and emission at 515 nm.

### Analysis

The *Preliminary FA Uptake Assay* data had to be normalized to account for varying CD36 expression levels as measured by GFPSpark expression. First, the average of the wells without cells (just the positive or negative buffer) was subtracted from the corresponding wells with cells to account for background. The values from the mutant CD36 wells, which received the negative buffer (values equivalent to GFPSpark expression), were divided by the average of the Wildtype CD36 wells to determine the ratio of GFPSpark expression. The inverse of this value was then

multiplied by the value of the wells with cells to determine the normalized FA uptake values. For example, if a well had 80% GFPSpark expression compared to Wildtype wells, the positive buffer well reading would be multiplied by 1/.8 before comparing to Wildtype. The average of the triplicates and the percent decrease compared to the Wildtype average were calculated.

#### FA Uptake Assay with BODIPY FL C16

HEK 293T/17 cells were plated in a 96 well tissue culture plate with six wells each of Untransfected, Wildtype, and K164Q cells, and grown to an average 80-90% confluency. A cell buffer was prepared with 1 ml 10x Hank's Balances Salt Solution (HBSS) (Gibco) (catalog number 14065-056), 9 ml sterile water (Sigma) (catalog number W4502-1L), and 0.1 g FA-free bovine serum albumin (BSA) (Alfa Aesar) (catalog number J64944). A boron dipyrromethene (BODIPY) solution was prepared with 4 ml cell buffer and 3.8  $\mu$ l of a 1 mg/ml BODIPY FL C16 (Molecular Probes) (catalog number D3821). A stop solution was prepared with 7 ml of phosphate buffered saline (PBS) and 0.014 g BSA and kept on ice. The medium was removed from the wells and replaced with 90  $\mu$ l cell buffer for three wells and 90  $\mu$ l BODIPY solution for the remaining three wells before incubation in the dark at room temperature for 5 minutes. 180  $\mu$ l of stop solution were added and incubated for 5 minutes. The solutions were replaced by a 90  $\mu$ l PBS overlay and the fluorescence endpoint was read using a Synergy H1 Hybrid Multi-Mode Reader (BioTek) with bottom optics, 100 gain, excitation at 485 nm, and emission at 515 nm.

#### Analysis

The raw data values for the wells which received the BODIPY solution were decreased by the average value of the same cell types that only received the cell buffer to account for GFPSpark expression and other background fluorescence. The average of the triplicates and the standard deviations were computed with Microsoft Excel for Mac (Version 16.29.1 (19091700)). A two-sample t-test assuming equal variances was applied with an alpha of 0.05 to determine if the different cell types were significantly different from each other.

#### Secretory Alkaline Phosphatase (SEAP) Assay

##### Cell Growth

All procedures were carried out in a level 2 biosafety cabinet with sterile materials. HEK-Blue mTLR2 cells were purchased from Invivogen (catalog number hkb-mtlr2). The cells were grown

in DMEM High Glucose supplemented with 10% heat inactivated FBS, 100 U/ml penicillin, 100 µg/ml streptomycin, and 1X HEK-Blue Detection (Invivogen) (catalog number hb-sel) on tissue culture plates in a 37°C incubator with 5% CO<sub>2</sub>. When cell growth reached 80-90% confluency, they were split to prevent overgrowth. The medium was discarded, the cells were resuspended in fresh medium, and transferred to a fifteen ml centrifuge tube. The plate was rinsed with fresh medium and this was also transferred to the previous centrifuge tube. The suspended cells were centrifuged at 300xg for 3 minutes. The supernatant was discarded, and the pellet resuspended in 2 ml of fresh medium. When carrying the cells in the same plate size, 500 µl were added to fresh medium so that they were plated at approximately 25% confluency. In some cases, the remaining cells were frozen with the addition of DMSO in a cryogenic tube and stored at -80°C.

### Transfection

HEK-Blue mTLR2 cells were plated at 25% confluency in a 96 well tissue culture plate. When cells were 50-60% confluent, they were transfected with plasmids using Lipofectamine 3000 Reagent (ThermoFisher Scientific) (catalog number L3000001). For each plasmid, in one microfuge tube, 55 µl of DMEM High Glucose and 1.65 µl Lipofectamine 3000 Reagent were mixed. In another microfuge tube, 55 µl of DMEM High Glucose, 1.1 µg of resuspended plasmid from *Plasmid Preparation*, and 2.2 µl of P3000 Reagent were mixed. The contents of the two microfuge tubes were combined and incubated for 15 minutes at room temperature. 10 µl of the solution were then added dropwise into each well and incubated at 37°C and 5% CO<sub>2</sub>. When the cells grew to 80-90%, they were used in the *SEAP Assay*.

### SEAP Assay

A 96 well plate with 6 wells each of HEK-Blue mTLR2 cells transfected with either the Wildtype CD36 plasmid, K164Q CD36 plasmid, or left untransfected, as well as six wells with just medium were used in this experiment. To three wells of each cell type, 15 µl of sterile water (very low endotoxin, Sigma) (catalog number W4502-1L) were added, and 15 µl of 300 ng/µl lipoteichoic acid (LTA) from *Staphylococcus aureus* (Sigma) (catalog number L2515-5MG) were added to the remaining three wells. The cells were then incubated overnight. 20µl of supernatant from each tissue culture well were transferred to 200 µl of prepared QUANTI-Blue (Invivogen) (catalog number rep-qb) in a separate 96 well bacterial plate. This plate was then

incubated for 1 hour before reading the optical density (OD) at 620 nm using a Synergy H1 Hybrid Multi-Mode Reader (BioTek). The cells then underwent the *Immunofluorescence* protocol to confirm the expression of CD36.

### Analysis

The data collected from the *SEAP Assay* were in triplicates. The average of the control wells was subtracted from the test wells. The average of the triplicates and the standard deviations were computed with Microsoft Excel for Mac (Version 16.29.1 (19091700)). A two-sample t-test assuming equal variances was applied with an alpha of 0.05 to determine if the different cell types were significantly different from each other.

### Immunofluorescence

Depending on well size, all volumes used in this procedure were sufficient to cover the cells fully. The medium was removed, and a 4% formaldehyde solution (Thermo Scientific) (catalog number 28908) in PBS was added for 10 minutes at room temperature to fix the cells. The cells were then washed with PBS. A 1:200 solution of CD36 (ME542) mouse monoclonal IgA antibody (Santa Cruz) (catalog number sc-13572) in PBS was added and incubated at room temperature for 1 hour. The cells were washed two times in PBS. A 1:200 solution of Goat pAb to MsIgA (Dylight 650) (Abcam) (catalog number ab97014) in PBS was added and incubated at room temperature in the dark for 1 hour. The cells were washed three times in PBS and a final overlaid with PBS was added. Cells were imaged with an EVOS Fl Digital Inverted Microscope (Advanced Microscopy Group) (catalog number AMF4300) under transmitted, GFP, and Cy5 channels.

### Bone Marrow Derived Macrophages (BMDM)

#### Endotoxin-free Plasmid Preparation

A pipette tip was used to scrape both K164Q and Wildtype plasmid containing DH5 $\alpha$  cells from the freeze downs prepared in *Plasmid Preparation* and transferred to flasks containing 30 ml LB broth supplemented with kanamycin and incubated overnight at 37°C with shaking at 250 rpm. The cultures were centrifuged at 6000xg for fifteen minutes at 4°C. The following protocol was performed with a QIAGEN EndoFree Plasmid Maxi Kit (catalog number 12362). The cell pellet

was resuspended in 10ml of Buffer P1 before adding 10 ml of Buffer P2 and vigorously inverting six times to mix. This was incubated at room temperature for 5 minutes. 10 ml of chilled Buffer P3 were added, mixed by vigorously inverting six times and transferred to the barrel of a QIAfilter cartridge with a cap on the nozzle. This solution was incubated at room temperature for 10 minutes before filtering the solution through the cartridge. 2.5 ml of Buffer ER were added to the filtered lysate and mixed by inverting before incubating on ice for 30 minutes. The solution was added to a QIAGEN-tip 500 that was previously equilibrated with 10 ml Buffer QBT and allowed to enter by gravity flow. The column was washed twice with 30 ml of Buffer QC and eluted with 15 ml of Buffer QN. The DNA was precipitated with 10.5 ml isopropanol and centrifuged at 17,000xg for 30 minutes at 4°C. The pellet was washed with 5 ml of endotoxin-free 70% ethanol and centrifuged at 17,000xg for 10 minutes at 4°C. The pellet was air-dried for 10 minutes and dissolved in endotoxin-free Buffer TE. All plasmid suspensions were analyzed for concentration and purity with a ThermoScientific NanoDrop 2000c Spectrophotometer (catalog number ND-2000C). Plasmid suspensions were also analyzed by gel electrophoresis to confirm concentration, purity, and size.

#### Collection of Bone Marrow

Tibias and femurs were collected from sacrificed CD36 knock out mice (University of Alberta animal use protocol AUC 0570). The bones were flushed with Iscove's Modified Dulbecco's Medium (IMDM) supplemented with 10% heat inactivated FBS, 100 U/ml penicillin, and 100 µg/ml streptomycin to collect the bone marrow. The cells ( $\sim 2 \times 10^7$ ) were centrifuged at 400xg for 5 minutes and resuspended in 4 ml FBS supplemented with 10 % DMSO and stored at -80°C in four cryogenic tubes per mouse.

#### Differentiation, Transfection, and Activation

One cryogenic tube of bone marrow from *Collection* was thawed in a 37°C water and diluted in 9 ml of RPMI (ThermoFisher Scientific) (catalog number 11875085) supplemented with 10% heat inactivated FBS, 100 U/ml penicillin, and 100 µg/ml streptomycin before spinning out the cells at 400xg for 5 minutes. The pellet was resuspended in 15 ml of Roswell Park Memorial Institute 1640 Medium (RPMI) supplemented with 10% heat inactivated FBS, 100 U/ml penicillin, 100 µg/ml streptomycin, and 16.6% L929 containing culture medium (LCCM) (prepared in house by another member of the lab) and plated on a 100mm bacterial petri dish.

L929 cells were purchased from ATCC (NCTC clone 929[L cell, L0929, derivative of strain L] (ATCC® CCL-1™)). L929 cells are a mouse fibroblast cell line that releases proteins and factors which promote the growth and differentiation of macrophages from total bone marrow<sup>61</sup>. The plate was incubated at 37°C and 5% CO<sub>2</sub>. After 4 days, the cells were fed with an additional 10 ml of differentiating medium and grown to confluency. Once confluent, the differentiating medium was removed by pipette. The cells were resuspended by pipetting into 4 ml of RPMI and transferred to a 15 ml centrifuge tube. An additional 3 ml of RPMI were used to pipette any remaining cells in the petri dish and added to the 15 ml centrifuge tube. The 15 ml centrifuge tube was centrifuged for 5 minutes at 200xg. The following transfection was completed with the Lonza Amaxa Mouse Macrophage Nucleofector Kit (Lonza) (catalog number VPA-1009). The cells were resuspended in 328 µl Mouse Macrophage Nucleofector Solution and 72 µl Supplement. To three aluminium cuvettes, 1 µg of *Endotoxin-free Plasmid* (Wildtype, K164Q) or endotoxin-free trisaminomethane ethylenediaminetetraacetic acid (TE) (negative) was added. 100 µl of the cell suspensions were transferred to each cuvette and program Y-001 on Amaxa Nucleofector Device II (Lonza) was utilized for transfection. The cuvette contents were diluted in 6 ml of RPMI supplemented with 10% heat inactivated FBS, 100 U/ml penicillin, and 100 µg/ml streptomycin, then 2 ml were transferred to 3x35 mm bacterial petri dishes. This results in 3 plates per plasmid condition (Wildtype, K164Q, Untransfected) so that each one plate per plasmid condition can undergo each activation condition (lipopolysaccharide (LPS), interleukin-4 (IL-4), no activator). 6 hours post transfection, 1 ml of RPMI supplemented with 10% heat inactivated FBS, 100 U/ml penicillin, 100 µg/ml streptomycin, and Recombinant Mouse IL-4 (carrier-free) (BioLegend) (catalog number 574304) was added to one plate per plasmid type so that the final IL-4 concentration was 10 ng/ml. 1 ml of RPMI supplemented with 10% heat inactivated FBS, 100 U/ml penicillin, 100 µg/ml streptomycin, and LPS from *Porphyromonas gingivalis* (1:1500 dilution prepared from ~10<sup>9</sup>/ml bacteria boiled for 10 minutes) was added to one plate per plasmid type. 1 ml of RPMI supplemented with 10% heat inactivated FBS, 100 U/ml penicillin, and 100 µg/ml streptomycin was added to one plate per plasmid type for a ‘no activator’ control. The plates were incubated at 37°C and 5% CO<sub>2</sub> overnight and then used in *Flow Cytometry*.

### Flow Cytometry

Activated cells from *Differentiation, Transfection, and Activation* were suspended in their medium, transferred to centrifuge tubes and centrifuged at 400xg for 4 minutes. The cells were resuspended in 200  $\mu$ l of PBS supplemented with 5% heat inactivated FBS. 100  $\mu$ l of this cell suspension were transferred to a 96-well V-bottom plate and incubated at room temperature for 15 minutes. The plate was centrifuged at 400xg for 4 minutes (all remaining centrifugations in this section under these conditions) and the supernatant was removed by plate inversion. Cells were resuspended in 100  $\mu$ l of the following antibodies in a 1:200 solution in PBS with 2% heat inactivated FBS: CD36 peridinin chlorophyll protein-cyanine 5.5 (PerCPCy5.5) (Santa Cruz) (catalog number SC-13572), F4/80 SuperBright 436 (Invitrogen) (catalog number 62-4801-82), cluster of differentiation 38 (CD38) allophycocyanin (APC) (Invitrogen) (catalog number 17-0381-82), and cluster of differentiation 163 (CD163) phycoerythrin (PE) (Invitrogen) (catalog number 12-1631-82). The suspension was incubated in the dark at room temperature for 30 minutes. The plate was centrifuged, inverted, pellets resuspended in 100  $\mu$ l PBS with 2% heat inactivated FBS and centrifuged again. The pellets were resuspended in 4% paraformaldehyde in PBS and incubated at room temperature in the dark for 10 minutes. The plate was centrifuged, inverted, pellets resuspended in 100  $\mu$ l PBS with 2% heat inactivated FBS and centrifuged again. The pellets were resuspended in 500  $\mu$ l of PBS with 2% FBS and kept on ice until analyzed by flow cytometry on the Attune NxT Acoustic Focusing Cytometer with channels BL1, BL3, RL1, VL1, and YL1. Mean fluorescence intensities were computed using FlowJo software after gating on the BMDM population using forward scatter versus side scatter.

### Modified Flow Cytometry

Activated cells from *Differentiation, Transfection, and Activation* were suspended in their medium, transferred to a centrifuge tube and centrifuged at 400xg for 4 minutes. The cells were resuspended in 200  $\mu$ l of PBS supplemented with 5% goat serum (Gibco) (catalog number 16210). 100  $\mu$ l of this cell suspension were transferred to a 96-well V-bottom plate and incubated at room temperature for 15 minutes. The plate was centrifuged at 400xg for 4 minutes (all remaining centrifugations in this section under these conditions) and the supernatant was removed by plate inversion. Cells were resuspended in 100 $\mu$ l of a 1:500 solution of CD36 PerCPCy5.5 antibody in PBS with 2% heat inactivated FBS. The suspension was incubated in

the dark at room temperature for 30 minutes. The plate was centrifuged, inverted, pellets resuspended in 100 $\mu$ l PBS with 2% FBS and centrifuged again. Cells were resuspended in 100  $\mu$ l of the following antibodies in a 1:500 solution in PBS with 2% heat inactivated FBS: F4/80 SuperBright 436, CD38 APC, and CD163 PE. The suspension was incubated in the dark at room temperature for 30 minutes. The plate was centrifuged, inverted, pellets resuspended in 100  $\mu$ l PBS with 2% heat inactivated FBS and centrifuged again. The pellets were resuspended in 4% paraformaldehyde in PBS and incubated at room temperature in the dark for 10 minutes. The plate was centrifuged, inverted, pellets resuspended in 100  $\mu$ l PBS with 2% heat inactivated FBS and centrifuged again. The pellets were resuspended in 500  $\mu$ l of PBS with 2% heat inactivated FBS and kept on ice until analyzed by flow cytometry on the Attune NxT Acoustic Focusing Cytometer with channels BL1, BL3, RL1, VL1, and YL1. Mean fluorescence intensities and histograms were computed using FlowJo software after gating on the BMDM population using forward scatter versus side scatter.

## Results

### K164Q Significantly Decreases FA Uptake by CD36

In this experiment, HEK293T/17 cells were transfected with a plasmid containing Wildtype CD36, CD36 with a single mutation at either F153 or K164, or left Untransfected. A preliminary FA uptake assay was performed with a commercial kit, then BODIPY FL C16 was utilized to confirm the mutation with the greatest decrease in FA uptake had a significant decrease. We used the HEK293T/17 cell line because it does not express detectable levels of proteins involved in FA uptake<sup>37</sup>. FA can passively diffuse across the cell membrane in this cell line, however, this value is similar across all transfection conditions, so any major changes in FA uptake can be attributed to the addition of Wildtype or mutated CD36. With the use of the commercial kit, the confluency between the groups was close, but not identical. We were able to take advantage of the reporter gene in the plasmid, GFP, to normalize the FA uptake data. Therefore, Untransfected cells were not included in the results because these cells did not contain GFP and the confluency could not be normalized along with the transfected groups.

From the eight mutations initially created and analyzed using a commercially available FA uptake kit, K164Q had the greatest decrease in FA uptake as compared to Wildtype CD36, with a 55.2% decrease (16675 RFU *vs* 37192 RFU, Table 4). K164R and F153A also showed inhibition, with a 48.8% and 46.8% decrease in FA uptake, respectively.

The decrease in FA uptake achieved by K164Q was further confirmed by measuring FA uptake using BODIPY FL C16, a labelled FA that is the same chain length as palmitic acid, whose uptake has been shown to be affected by CD36 expression<sup>62</sup>. The CD36 K164Q mutant had a 45.7% decrease in FA uptake compared to Wildtype CD36 ( $18107 \pm 2667.4$  RFU *vs*  $33330 \pm 2457.9$  RFU,  $p=0.002$ , Figure 6). Cells expressing K164Q did not have significantly different FA uptake as compared to Untransfected cells ( $18107 \pm 2667.4$  RFU *vs*  $19071 \pm 2815.1$  RFU,  $p=0.689$ , Figure 6). As expected, Untransfected cells had significantly decreased FA uptake compared to cells expressing Wildtype CD36 ( $19071 \pm 2815.1$  RFU *vs*  $33330 \pm 2457.9$  RFU,  $p=0.003$ , Figure 6).

Table 4. Percent decrease in FA uptake using a FA Uptake Kit. Values normalized to GFP expression and percent decrease refers to the comparison of cells expressing a mutant CD36 to cells expressing Wildtype CD36 after one hour

Mutation	Average Normalized RFU	Percent Decrease
K164R	19054	48.8
K164Q	16675	55.2
K164Y	27292	26.6
F153N	46488	-25.0
F153W	28526	23.3
F153A	19778	46.8
Wildtype	37192	0

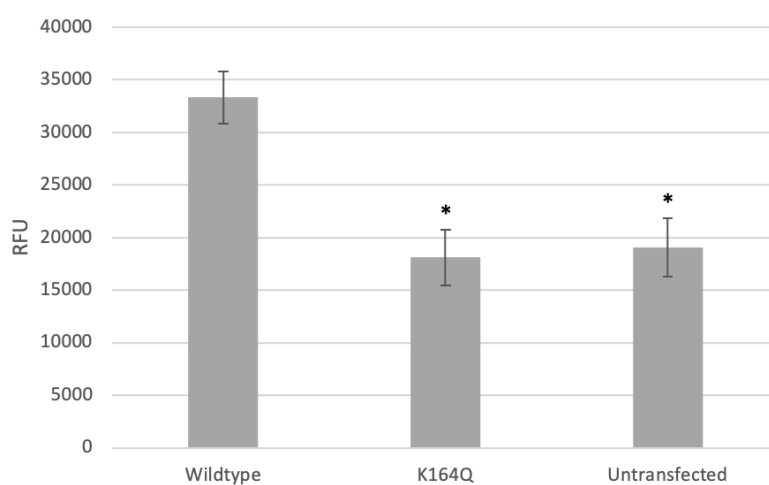


Figure 6. FA Uptake Assay with BODIPY FL C16, 5-minute time point \* $p < 0.05$  compared to Wildtype

K164Q does not significantly impact CD36 signaling in response to LTA

The first aim of this project was to identify a single amino acid mutation that does not disrupt the expression of CD36, decreases LCFA uptake, and does not disrupt CD36 signalling. We chose

signaling as a representative of normal functionality independent of FA uptake because signaling is a major role of CD36, including in response to thrombospondin-1 and DAMPs. A SEAP assay using HEKBlue cells expressing toll like receptor 2 (TLR2) was chosen to analyze CD36's signalling capabilities. CD36 is a known coreceptor for TLR2 in response to LTA.

As shown in Figure 7, SEAP expression was not significantly different between cells expressing the K164Q mutant and cells expressing Wildtype CD36 ( $1.6436 \pm 0.102$  OD vs  $1.679 \pm 0.163$

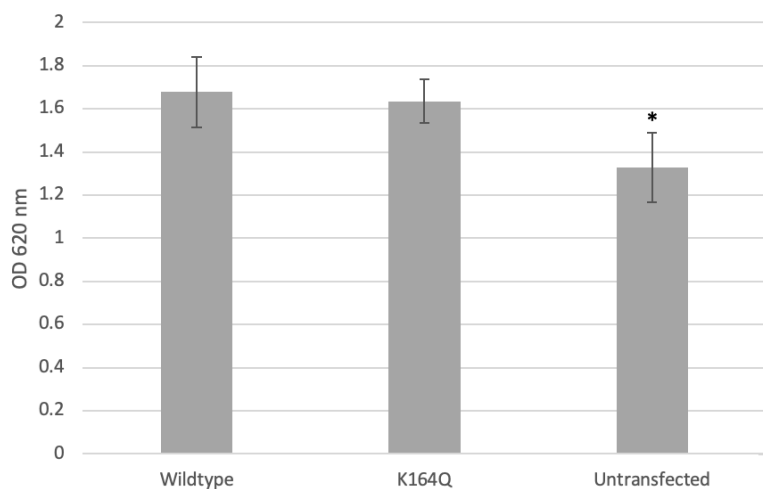


Figure 7. SEAP assay using QUANTI-Blue incubated for one hour after cells in presence of LTA overnight, \* $p < 0.05$  compared to K164Q

OD,  $p = 0.718$ , Figure 7). The K164Q CD36 mutant had a statistically significant difference in SEAP expression compared to Untransfected cells ( $1.6436 \pm 0.102$  OD vs  $1.329 \pm 0.161$  OD,  $p = 0.049$ , Figure 7).

### BMDM M2 Phenotype

Expression May be Dependent on CD36 Mediated FA Uptake

The second aim of this project was

to determine if the exclusive loss of LCFA transport by CD36 has biological effects in terms of macrophage phenotype. CD36 is a marker for M2 macrophage, but it is not known if the uptake of LCFA by CD36 is essential for M2 activation. Murine BMDM were transfected with Wildtype CD36, K164 CD36, or left Untransfected and activated with LPS (for M1), IL-4 (for M2), or not activated. The phenotypes of the cells were then analyzed for expression of CD38 and CD163, markers for M1 and M2, respectively, by flow cytometry.

The MFIs from *Flow Cytometry* did not show patterns consistent with plasmid transfection. GFP is shown in Figure 8 and was expected to be lowest in Untransfected cells and to show different expression, based on transfection efficiency in those cells receiving plasmid. CD36 expression is shown in Figure 9 and is also inconsistent with what would be expected based on the plasmid transfected. We would expect that GFP and CD36 expression levels would be equal across Wildtype and K164Q, all being higher than Untransfected. For CD38 expression (Figure 11), we would expect that Wildtype CD36 activated with LPS would have the highest expression as this procedure should produce a population of M1 macrophages. As shown in Figure 10, cells that have been transfected with K164Q have lower F4/80 expression compared to those transfected with Wildtype or Untransfected ( $11947 \pm 600$  MFI vs  $17606 \pm 1422$  MFI and  $16210 \pm 650$  MFI, respectively). F4/80 is a marker for murine macrophages, so should be equal across all samples as they were all differentiated with LCCM. As shown in Figure 12, comparing the samples that

were activated by IL-4 (to induce an M2 phenotype), there was a decrease in CD163 expression in the samples transfected with Wildtype CD36 compared to those transfected with K164Q (2825 MFI vs 1103 MFI), while the Wildtype and K164Q samples under different activation conditions had similar results. Untransfected cells activated by IL-4 had CD163 expression in between the Wildtype and K164Q (1848 MFI). Due to the unexpected expression of the markers GFP and CD36, the remaining data cannot be confirmed without optimization.

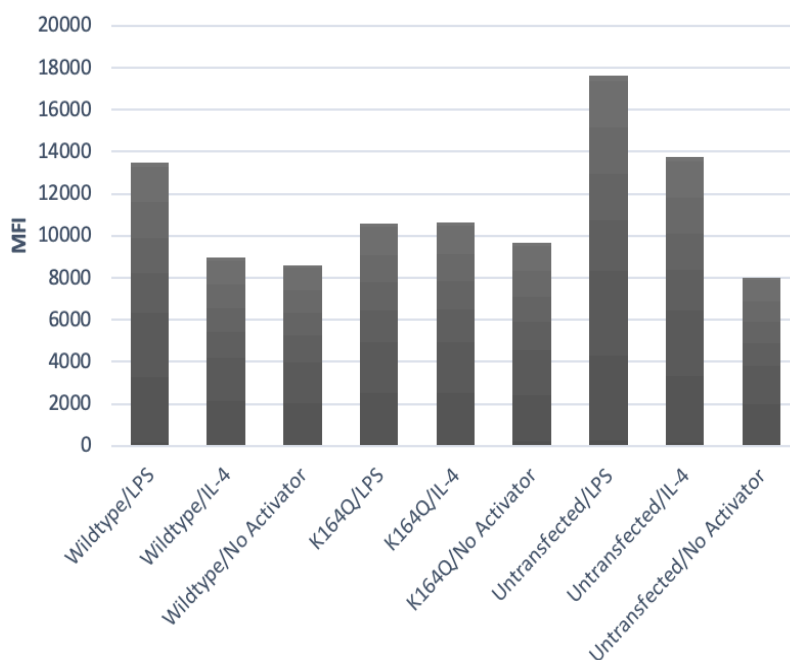


Figure 8. MFIs of BMDM in the BL1 channel of the Attune NxT Acoustic Focusing Cytometer representing GFP expression from *Flow Cytometry* protocol

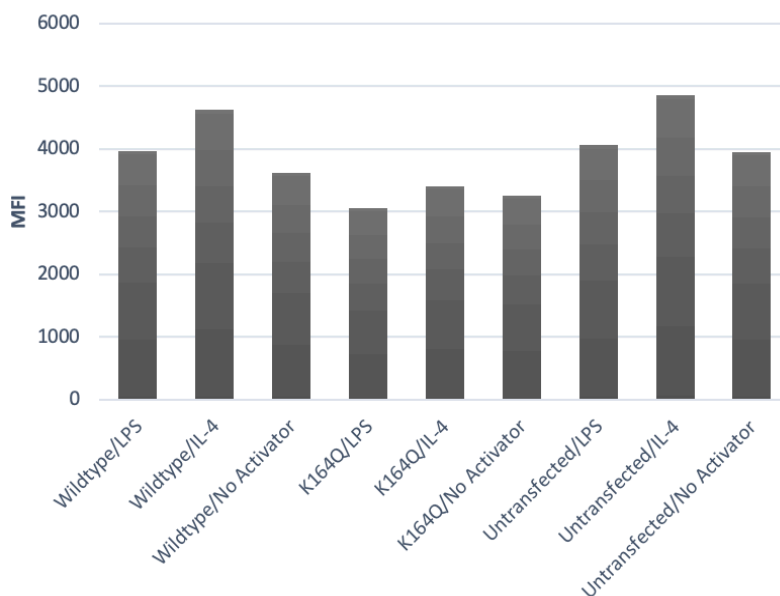


Figure 9. MFIs of BMDM in the BL3 channel of the Attune NxT Acoustic Focusing Cytometer representing CD36 expression with a PerCP-Cy5.5 antibody from *Flow Cytometry* protocol

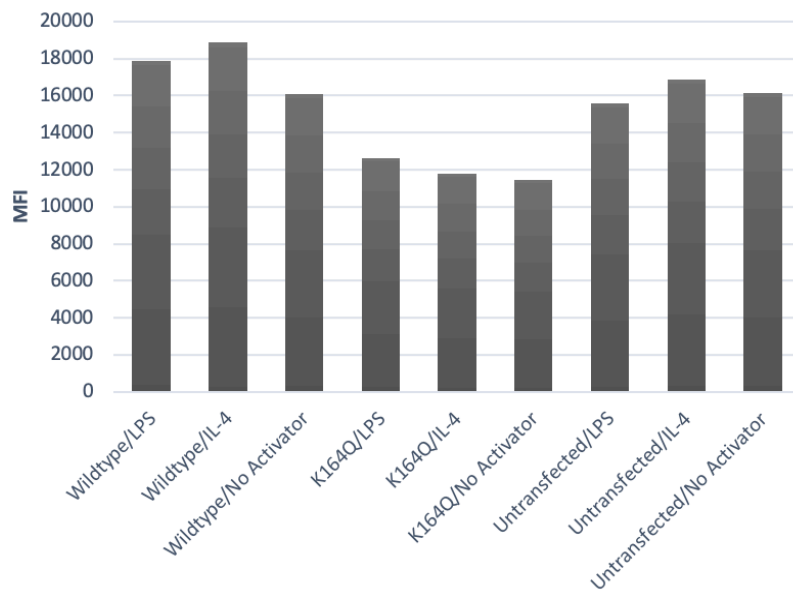


Figure 10. MFIs of BMDM in the VL1 channel of the Attune NxT Acoustic Focusing Cytometer representing F4/80 expression with a SuperBright 436 antibody from *Flow Cytometry* protocol

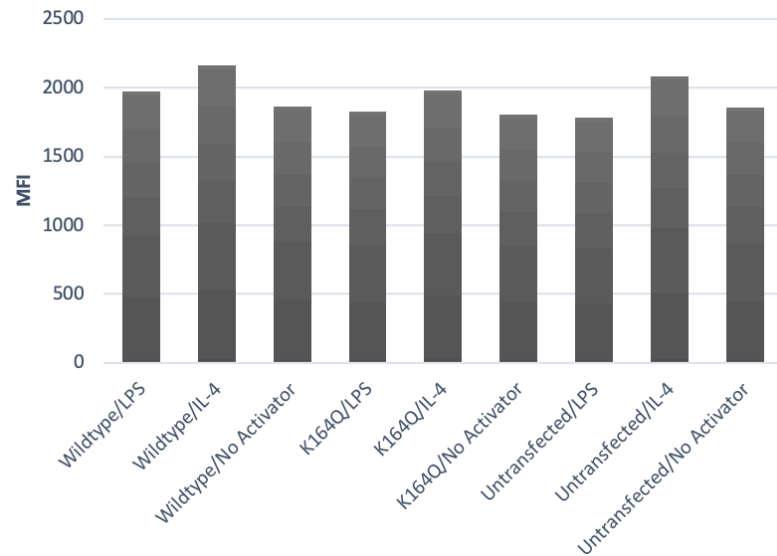


Figure 11. MFIs of BMDM in the RL1 channel of the Attune NxT Acoustic Focusing Cytometer representing CD38 expression with an APC antibody from *Flow Cytometry*

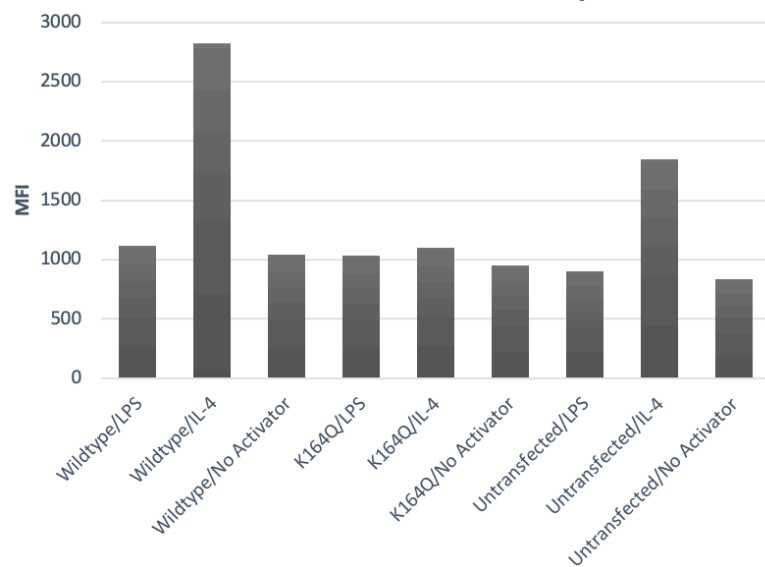


Figure 12. MFIs of BMDM in the YL1 channel of the Attune NxT Acoustic Focusing Cytometer representing CD163 expression with a PE antibody from *Flow Cytometry* protocol

## Amaxa Nucleofector System Does Not Produce a High Transfection Efficiency

In an attempt to optimize the flow cytometry experiment so that expected results were achieved, the blocking procedure, concentration of antibody solutions, and order of antibody staining were changed. The MFIs from *Modified Flow Cytometry* did not show patterns consistent with plasmid transfection in the case of CD36 (Figure 14), F4/80 (Figure 15), CD38 (Figure 16), and CD163 (Figure 17). These experiments were performed using instructions from Amaxa for transfection of primary macrophages using the Nucleofector System. Figure 13 shows cells transfected with Wildtype ( $88.4 \pm 1.9$  MFI) and K164Q ( $92.3 \pm 1.8$  MFI) had higher GFP expression compared to Untransfected cells ( $48.6 \pm 0.9$  MFI). Examination of the histograms of GFP expression shows that 0.59% of Untransfected cells have GFP expression above the threshold RFU (Figure 20), while Wildtype has 5.80% (Figure 18) and K164Q has 6.42% (Figure 19). This suggests that the inaccuracies observed in the data presented as MFI may be due to low transfection.

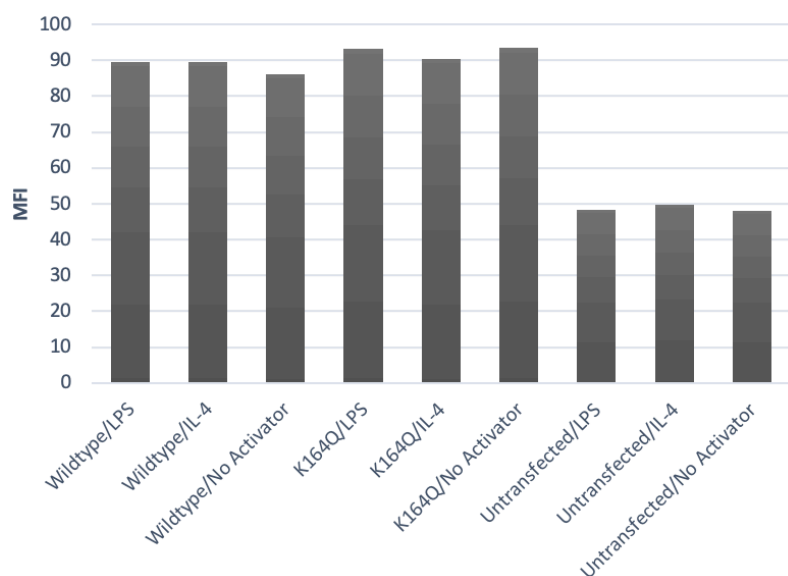


Figure 13. MFIs of BMDM in the BL1 channel of the Attune NxT Acoustic Focusing Cytometer representing GFP expression from *Modified Flow Cytometry* protocol

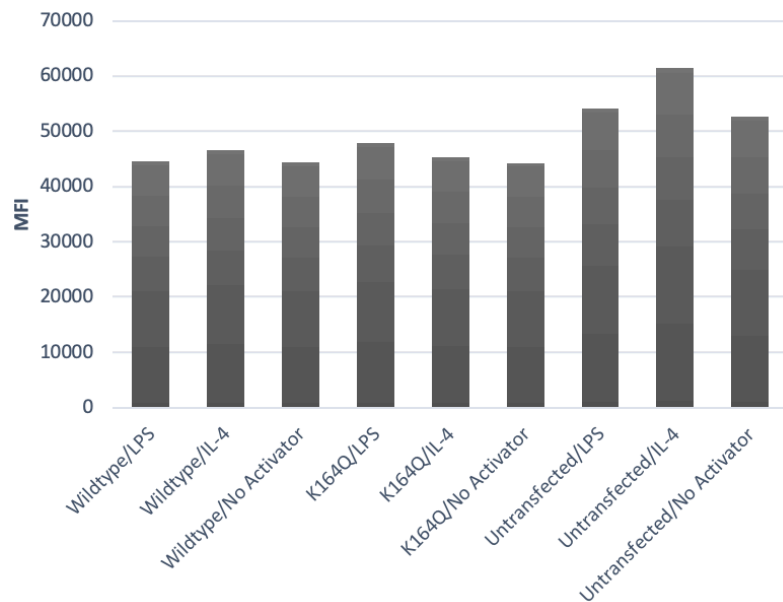


Figure 14. MFIs of BMDM in the BL3 channel of the Attune NxT Acoustic Focusing Cytometer representing CD36 expression with a PerCP-Cy5.5 antibody from *Modified Flow Cytometry* protocol

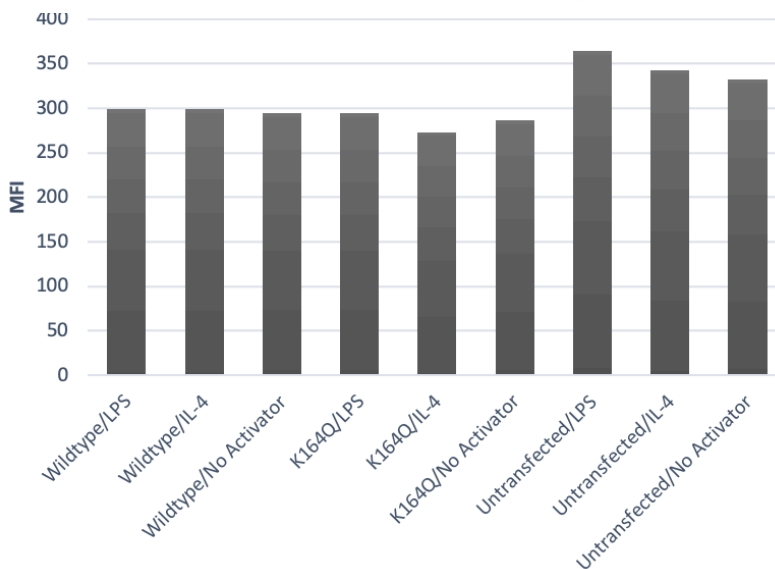


Figure 15. MFIs of BMDM in the VL1 channel of the Attune NxT Acoustic Focusing Cytometer representing F4/80 expression with a SuperBright 436 antibody from *Modified Flow Cytometry* protocol

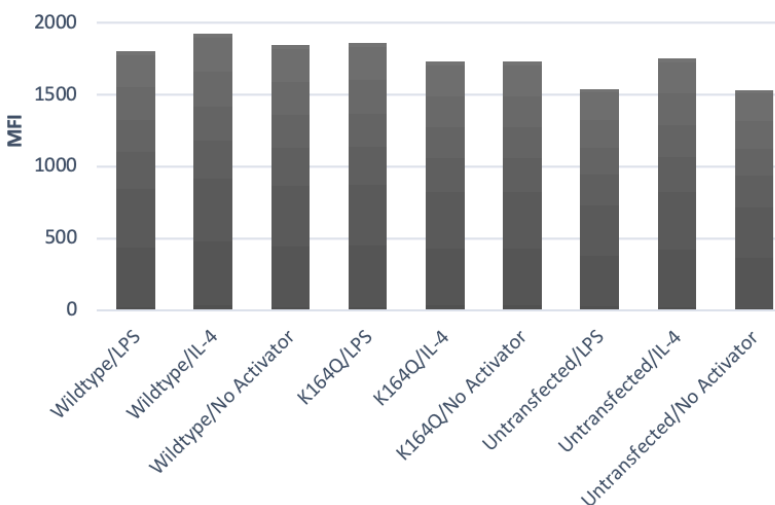


Figure 16. MFIs of BMDM in the RL1 channel of the Attune NxT Acoustic Focusing Cytometer representing CD38 expression with an APC antibody from *Modified Flow Cytometry* protocol

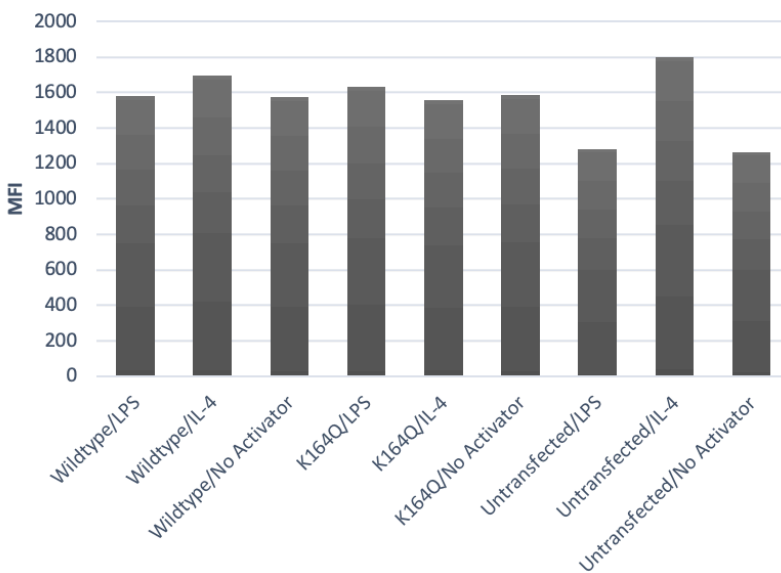


Figure 17. MFIs of BMDM in the YL1 channel of the Attune NxT Acoustic Focusing Cytometer representing CD163 expression with a PE antibody from *Modified Flow Cytometry* protocol

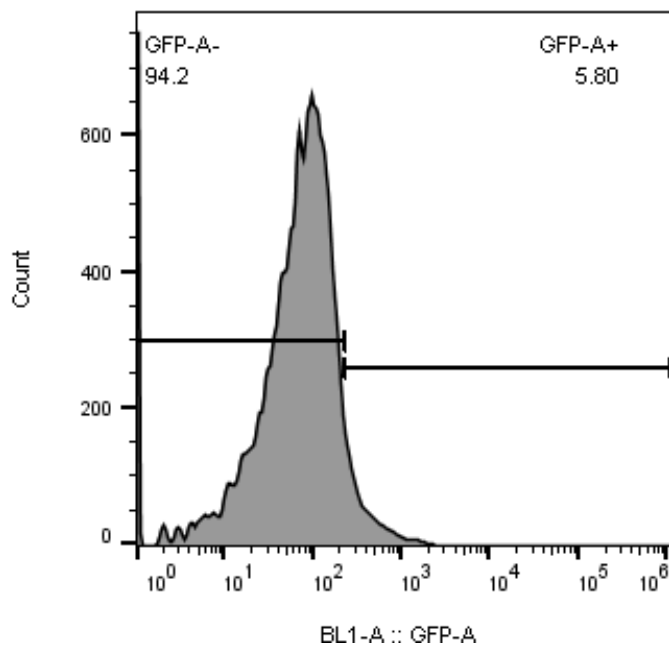


Figure 18. Histogram of BMDM transfected with Wildtype and activated by IL-4 in the BL1 channel of the Attune NxT Acoustic Focusing Cytometer representing GFP expression from *Modified Flow Cytometry* protocol

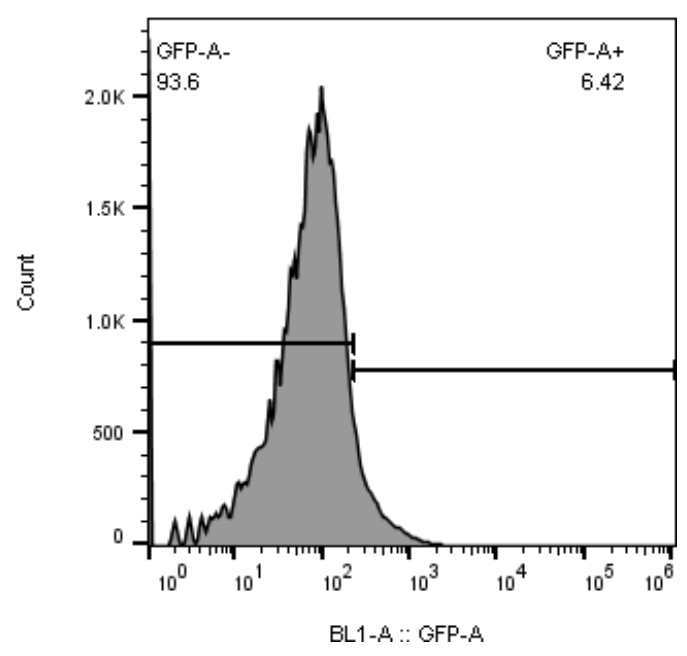


Figure 19. Histogram of BMDM transfected with K164Q and activated by IL-4 in the BL1 channel of the Attune NxT Acoustic Focusing Cytometer representing GFP expression from *Modified Flow Cytometry* protocol

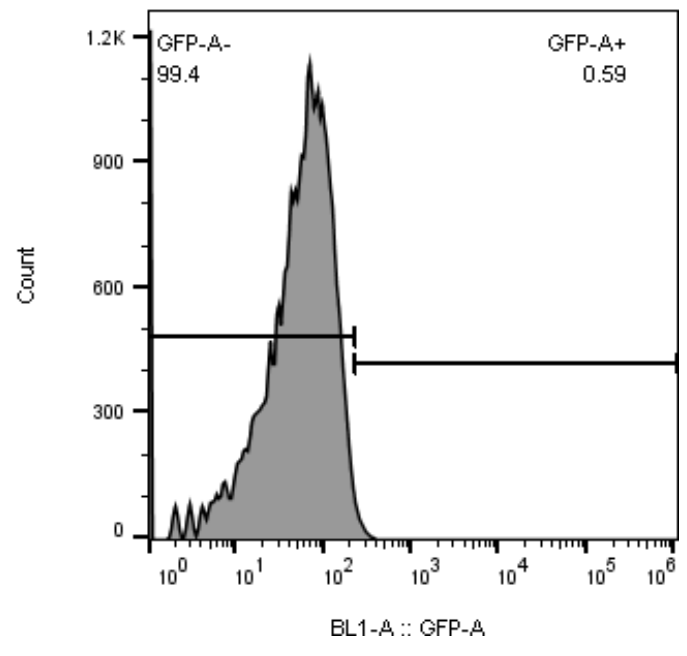


Figure 20. Histogram of Untransfected BMDM activated by IL-4 in the BL1 channel of the Attune NxT Acoustic Focusing Cytometer representing GFP expression from *Modified Flow Cytometry* protocol

## Discussion

This research project was undertaken in hopes of determining if a single point mutation in CD36 exclusively decreases LCFA uptake and if the loss of that function skews macrophages to an M1 phenotype. The goal was to identify an amino acid that played a critical role in cellular FA uptake by CD36 through site-specific mutagenesis. The outcome measures were that CD36 exclusively loses its ability to transport LCFA while preserving other functions and assessment of the impact of this mutation on macrophage phenotypes. Based on the literature, two sites previously identified through structural modelling as playing a role in FA uptake by CD36, F153 and K164, were initially analyzed. Our analysis showed the mutation of K164Q was the best mutant for further studies. We achieved the objective to identify a mutant that blocks FA uptake while preserving signalling but were unable to complete the aim to transfect this mutant, K164Q, into primary macrophages and determine the impact on phenotype.

### K164Q Significantly Decreases LCFA Uptake by CD36

The Fatty Acid Uptake Kit by Sigma-Aldrich that was used for the preliminary FA uptake assay was chosen for its user-friendly setup and analysis which were desirable when preparing and running 54 samples. This kit was able to give some guidance as to which mutants had the largest decrease in FA uptake (Table 4), but it uses a dodecanoic acid (also known as lauric acid) fluorescent FA substrate. Dodecanoic acid is considered a MCFA<sup>63</sup> and therefore, does not suffice to conclude that this mutant fulfills our criteria in terms of LCFA. The largest decrease in FA uptake was found with the mutant K164Q (Table 4) and this mutant was further studied with the second method of FA uptake.

The FA uptake assay with BODIPY FL C16 provided the freedom to choose a long chain, 16 carbon chain FA derivative. Although slightly more time consuming to set up and run, there were fewer samples to deal with thanks to the previous narrowing of the field of mutants. The BODIPY FL C16 method confirmed that K164Q results in a large drop in FA transport, specifically a significant drop of 45.7% (Figure 6). This result does not specifically prove that the mutation prevents the transport itself, but more likely prevents the initial binding of LCFA to CD36 before the transport can occur. Previous work looking at this specific site in regard to oxidized phosphatidylcholine and oxidized LDL binding reported mutating K164 to alanine or

glutamic acid prevented binding <sup>64</sup>; this may be the case here, but specific binding assays would have to be completed. These findings fit with Pascuals et al.'s findings in 2017 where comparisons between Wildtype CD36, K164A, and endogenous CD36 depletion in tumour cells found the K164A mutant and the endogenous CD36 depletion cells had similar lipid droplet formations <sup>65</sup>.

Wildtype CD36 has a lysine residue at position 164 and this residue has a positive charge (Figure 21). The passage of LCFA from the extracellular environment, through CD36, may involve an interaction between the positive lysine and the negative carboxyl end of LCFA, which would be interrupted by the replacement of the neutral glutamine. This charge change may also impact interactions with neighbouring side chains, slightly altering the structure and physically impacting the transport of LCFA. This residue does not lie in the core of the protein, so major structural changes impacting other functions are not expected.

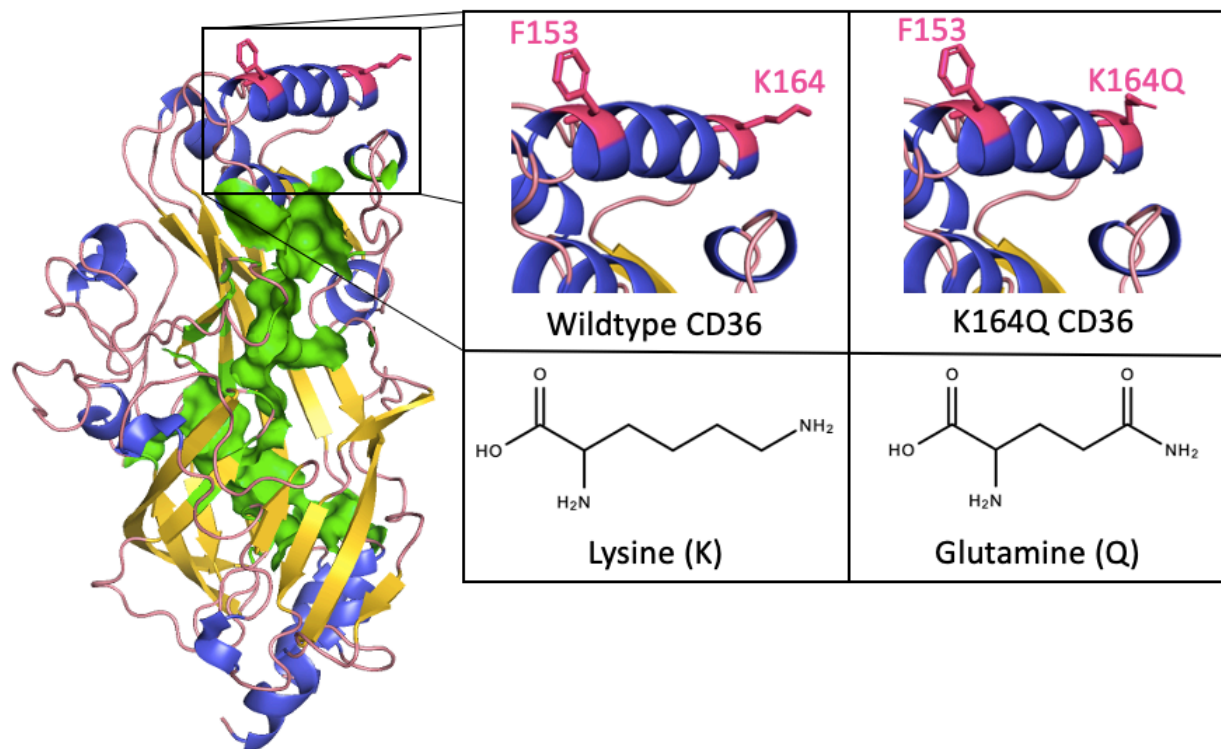


Figure 21. Structural modelling of Wildtype and K164Q CD36 with fatty acid binding sites in green created with The PyMOL Molecular Graphics System, V 2.4.0 (Provided by Zahra Mantaka, unpublished) and chemical structures of lysine and glutamine

## K164Q Does Not Significantly Impact CD36 Signaling in Response to LTA

The method used to analyze signalling by CD36 relies on activation of the nuclear factor kappa light chain enhancer of activated B cells (NF- $\kappa$ B) pathway by LTA. The cell line that was used expressed TLR2, which will activate the NF- $\kappa$ B pathway by itself when introduced to LTA <sup>66</sup>, which is why Untransfected cells had a reading above zero for the SEAP assay (Figure 7). CD36 is a known co-receptor for TLR2 which has been demonstrated to increase NF- $\kappa$ B activation in response to LTA <sup>66</sup>, which is represented as the increase in SEAP for Wildtype CD36 (Figure 7). The similar values between Wildtype CD36 and K164Q CD36 suggests the K164Q mutation does not significantly impact signaling by CD36 (Figure 7).

Our current findings contradict those from Xu et al. <sup>37</sup> suggesting CD36 promotes an increase in esterification, possibly through signalling or interactions with enzymes, and does not independently uptake LCFA. This conclusion was drawn after observing that cells expressing wildtype CD36 or left untransfected had the same rate of LCFA transfer, but the presence of CD36 increased esterification and therefore increased the proportion of FA stored as triacylglycerols and monoglycerols. This project has demonstrated that even when our mutant CD36 is capable of signalling, we can observe a decrease in overall LCFA uptake, regardless of their downstream fate. If it were signalling by CD36 which was responsible for increasing esterification within the cell, then this would not have been possible.

The finding that K164Q CD36 does not have impaired signalling compared to Wildtype CD36 suggests that the signalling capabilities of CD36 were not compromised. All signalling activated by an extracellular ligand is predicted to originate from one location, the intracellular C-terminal domain <sup>19</sup>. Intact signalling capabilities also confirms correct protein folding and allocation to the membrane. The LCFA uptake assay alone could not prove this as the decrease in LCFA uptake could have been due to CD36 not being present on the membrane and/or being misfolded. We can now deduce that the decrease in LCFA uptake was solely because of the mutated lysine residue.

## BMDM M2 Phenotype Expression May be Dependent on CD36 Mediated LCFA Uptake

The flow cytometry experiment analyzed GFP, CD36, F4/80, CD38, and CD163. GFP was analyzed as an indirect measure of CD36 expression as it was transfected into the cell on the same plasmid. GFP was present in the cell samples before antibody staining and could not be eliminated before analysis so was included in the readings as a control. It was expected that the Wildtype and K164Q samples would have all similar GFP expression (Figure 8), all being higher than the Untransfected samples, regardless of activator. A similar pattern was expected with CD36 expression (Figure 9), but this was not observed. F4/80 was chosen as a marker for murine macrophages<sup>67</sup> to assist in selecting the correct population of cells for analysis and confirming differentiation. The expected result for F4/80 expression was similar readings across all samples (Figure 10). CD38 was used as a marker for M1 expression<sup>68</sup> and was predicted to be upregulated in samples activated with LPS; however, this was not the case (Figure 11). CD163 was used as a marker for M2 expression<sup>69</sup> and predicted to be upregulated in the Wildtype sample activated by IL-4 and downregulated in samples activated by LPS or no activator. In this case, an increase in CD163 in the Wildtype sample was observed, suggesting the activation by IL-4 produced an M2 population of macrophages (Figure 12). The K164Q sample activated by IL-4 had similar levels to the K164Q samples activated with LPS or nothing, suggesting that the lack of LCFA transport provided by CD36 prevented M2 expression in macrophages. The Untransfected cells activated with IL-4 had CD163 levels in between Wildtype and Untransfected. This perhaps suggests that the presence of CD36 without the ability to transport LCFA not only prevents M2 expression, but actually restricts the cells' ability to become M2 more than if CD36 was completely absent. With unexpected results for the controls in this experiment, these findings are tentative only and should cautiously be viewed until repeated.

## Amxa Nucleofector System Does Not Produce High Transfection Efficiency

The repeated flow cytometry experiment allowed the chance to change the blocking and staining of BMDM to help determine if they were causing the deviations from expected results in the controls noted above. The expected results remained the same in this experiment. Similar to above, no distinct patterns were observed in CD36 (Figure 14), F4/80 (Figure 15), or CD38 (Figure 16) expression levels. The distinct differences previously observed in CD163 expression

were no longer present (Figure 17), but a new pattern has emerged. The expression levels of GFP were as expected, with Wildtype and K164Q samples higher than Untransfected samples (Figure 13).

A variety of possibilities were discussed as to why the expected results were still not observed, including cell death and non-specific binding; some clarity on the issue was found when looking at the histograms for GFP. Although the Wildtype and K164Q transfected cells had an overall increase in MFI compared to the Untransfected samples (Figure 13), the number of cells within the samples that registered as a positive reading only came out to 5.80% (Figure 18) and 6.42% (Figure 19), respectively. The number of cells in the Untransfected samples that registered as positive for GFP under the same conditions was 0.59% (Figure 20). With such a low number of cells transfected, this explains the lack of patterns observed in the MFI data. This matter could not be further addressed due to time constraints and restricted lab access due to COVID-19. Highly qualified personnel in the Febbraio Lab will continue to develop a protocol that will provide trusted results on the impact LCFA transport by CD36 has on macrophage phenotype expression.

## Limitations

The reported findings of this research must be taken in consideration of its limitations. For the LCFA uptake and SEAP assay, it was assumed that Wildtype CD36 and K164Q CD36 had equal expression. This assumption was made because the genes were in the same plasmid backbone, containing the same promoter, and GFP expression was confirmed by microscopy for both. However, a quantitative protein expression analysis was not performed to confirm similar enough expression levels not to impact the results of the following assays. Within the LCFA uptake assay, we did not perform separate binding and transport assays, just overall uptake into the cells. Therefore, when it is stated that transport has decreased, it does not necessarily mean the transport mechanism has been impacted, it could be an impact in the initial binding of LCFA to CD36. The ultimate limitation to any *in vitro* experiment is that the results cannot be directly implied to be true within a living system. CD36 that is expressed within human tissues is affected by many more variables than could be introduced within an *in vitro* model, including other transporters, activators, receptors, and ligands.

## Clinical Opportunities

The World Health Organization estimates that 1.9 billion, or 39% of adults, were overweight in 2016, and this number is climbing <sup>70</sup>. In 2019, 38 million children under 5 years old were overweight, and this increases their chances of remaining overweight in adulthood <sup>70</sup>. Being overweight is associated with developing cardiovascular diseases, type 2 diabetes, musculoskeletal disorders, cancer, and an overall higher mortality rate <sup>70</sup>. In Canada, the economic costs associated with obesity are rising, with the latest report from 2008 reaching \$4.6 billion <sup>71</sup>.

It has been demonstrated through heterozygous CD36 deficient human subjects that a decrease in CD36 expression infers protection against developing obesity and metabolic syndrome with increased high-density lipoproteins and decreased triglycerides <sup>38</sup>. Previous therapeutic treatments have been shown to decrease expression of CD36, including atorvastatin in platelets <sup>72</sup> and pitavastatin in monocytes and macrophage <sup>73</sup>. This research identifies a new target for the development of a CD36 specific therapeutic, lysine 164. The creation of a short acting small molecule inhibitor would allow CD36 to function normally day to day, performing its important functions as a scavenger receptor and thrombospondin receptor, but with the ability to inhibit LCFA transport in times of high circulating levels, postprandial for example. This would help prevent the development of increased fat storage, leading to obesity and metabolic syndrome.

## Future Directions

Of utmost importance regarding this research would be to optimize the protocols to produce evidence that the lack of LCFA uptake by CD36 on BMDM would prevent an M2 phenotype expression. Steps to do so would require increased transfection efficiency of the Wildtype and K164Q plasmids, perhaps through the use of adenoviruses. An optimized protocol for analyzing M2 markers would also have to be created. If this is continued through the use of flow cytometry, the antibody staining protocol and machine settings would have to be optimized. Another method of analyzing M2 markers would be through real-time PCR quantifying mRNA expression in macrophage. Similar *in vitro* experiments can be performed to determine the impact of CD36 LCFA uptake in various cell types, including adipocytes and endothelial cells.

If proven that LCFA uptake is essential for M2 expression, more can be learnt by expressing K164Q CD36 in a mouse model. This can be accomplished through a transgenic mouse model or with the use of CRISPR/Cas9 technology. The process of wound healing, which relies heavily on M2 macrophages<sup>74</sup> would be of interest comparing Wildtype, K164Q, and total knock out mice. Many factors, including circulating triglycerides, inflammation markers, and adipose tissue, can be compared to elucidate the specific effects of LCFA uptake by CD36 apart from signalling. Tissue resident macrophages could also be analyzed to determine if the prevention of M2 expression is also accomplished *in vivo*. If it is not, perhaps the increase in activators present *in vivo*, which were not introduced *in vitro*, also play a major role.

## Conclusion

The study of CD36 and LCFA uptake continues to be an important endeavour due to the importance of LCFA in our cells and its connection to various conditions including obesity, diabetes, and cardiovascular disease. This project aimed to identify a single amino acid mutation that does not disrupt the expression of CD36 or its ability to signal while decreasing LCFA uptake, then determining if that mutation has biological effects in macrophage phenotype expression. Through two different methods, we demonstrated that the mutation K164Q significantly decreased LCFA uptake *in vitro* in HEK293T/17 cells. This mutation did not significantly decrease the signaling capabilities of CD36, as demonstrated through a SEAP assay. Low transfection efficiency prevented a conclusion on the impact on macrophage phenotype, but the collected data suggest this can be proven in the near future with an optimized protocol. This project encourages future work in the topic by confirming decreased M2 expression in macrophages without the LCFA uptake by CD36 and opens up the possibility of examining the exclusive loss of CD36 LCFA uptake in a mouse model where previous study only examined CD36 knockouts.

## References

1. Schönfeld P, Wojtczak L. Short- and medium-chain fatty acids in energy metabolism: the cellular perspective. *Journal of lipid research*. 2016;57(6):943-954. doi: 10.1194/jlr.r067629.
2. Sassa T, Kihara A. Metabolism of Very Long-Chain Fatty Acids: Genes and Pathophysiology. *Biomolecules & therapeutics*. 2014;22(2):83-92. doi: 10.4062/biomolther.2014.017.
3. Carta G, Murru E, Banni S, Manca C. Palmitic Acid: Physiological Role, Metabolism and Nutritional Implications. *Frontiers in physiology*. 2017;8:902. doi: 10.3389/fphys.2017.00902/full.
4. Raatz SK, Conrad Z, Jahns L, Belury MA, Picklo MJ. Modeled replacement of traditional soybean and canola oil with high-oleic varieties increases monounsaturated fatty acid and reduces both saturated fatty acid and polyunsaturated fatty acid intake in the US adult population. *The American journal of clinical nutrition*. 2018;108(3):594-602. doi: 10.1093/ajcn/nqy127.
5. Tutunchi H, Ostadrahimi A, Saghafi-Asl M. The Effects of Diets Enriched in Monounsaturated Oleic Acid on the Management and Prevention of Obesity: a Systematic Review of Human Intervention Studies. *Advances in nutrition*. 2020;11(4):864-877. doi: 10.1093/advances/nmaa013.
6. Glatz JFC, Luiken, Joost J. F. P, Bonen A. Membrane Fatty Acid Transporters as Regulators of Lipid Metabolism: Implications for Metabolic Disease. *Physiological reviews*. 2010;90(1):367-417. doi: 10.1152/physrev.00003.2009.

7. Schaffer JE, Lodish HF. Expression cloning and characterization of a novel adipocyte long chain fatty acid transport protein. *Cell*. 1994;79(3):427-436. doi: 10.1016/0092-8674(94)90252-6.
8. Anderson CM, Stahl A. SLC27 fatty acid transport proteins. *Molecular aspects of medicine*. 2013;34(2-3):516-528. doi: 10.1016/j.mam.2012.07.010.
9. CD36 CD36 molecule [ Homo sapiens (human) ].  
<https://www.ncbi.nlm.nih.gov/gene?Db=gene&Cmd=DetailsSearch&Term=948>. Accessed August 17, 2020.
10. Abumrad N, el-Maghrabi M, Amri E, Lopez E, Grimaldi P. Cloning of a rat adipocyte membrane protein implicated in binding or transport of long-chain fatty acids that is induced during preadipocyte differentiation. Homology with human CD36. *Journal of Biological Chemistry*. 1993;268(24):17665.
11. Clemetson KJ, Pfueller SL, Luscher EF, Jenkins CS. Isolation of the membrane glycoproteins of human blood platelets by lectin affinity chromatography. *Biochimica et biophysica acta*. 1977;464(3):493.
12. PrabhuDas MR, Baldwin CL, Bollyky PL, et al. A Consensus Definitive Classification of Scavenger Receptors and Their Roles in Health and Disease. *The Journal of immunology (1950)*. 2017;198(10):3775-3789. doi: 10.4049/jimmunol.1700373.

13. Fagerberg L, Hallström BM, Oksvold P, et al. Analysis of the Human Tissue-specific Expression by Genome-wide Integration of Transcriptomics and Antibody-based Proteomics. *Molecular & cellular proteomics*. 2014;13(2):397-406. doi: 10.1074/mcp.m113.035600.
14. Duff MO, Olson S, Wei X, et al. Genome-wide identification of zero nucleotide recursive splicing in *Drosophila*. *Nature*. 2015;521(7552):376-379. doi: 10.1038/nature14475.
15. Belz GT, Vremec D, Febbraio M, et al. CD36 Is Differentially Expressed by CD8+ Splenic Dendritic Cells But Is Not Required for Cross-Presentation In Vivo. *The Journal of Immunology*. 2002;168(12):6066-6070. doi: 10.4049/jimmunol.168.12.6066.
16. Yang X, Okamura DM, Lu X, et al. CD36 in chronic kidney disease: novel insights and therapeutic opportunities. *Nature reviews. Nephrology*. 2017;13(12):769-781. doi: 10.1038/nrneph.2017.126.
17. Silverstein R, Baird M, Lo S, Yesner L. Sense and antisense cDNA transfection of CD36 (glycoprotein IV) in melanoma cells. Role of CD36 as a thrombospondin receptor. *Journal of Biological Chemistry*. 1992;267(23):16607.
18. Osz K, Ross M, Petrik J. The thrombospondin-1 receptor CD36 is an important mediator of ovarian angiogenesis and folliculogenesis. *Reproductive biology and endocrinology*. 2014;12(1):21. doi: 10.1186/1477-7827-12-21.
19. Silverstein RL, Li W, Park YM, Rahaman SO. Mechanisms of cell signaling by the scavenger receptor CD36: implications in atherosclerosis and thrombosis. *Transactions of the American Clinical and Climatological Association*. 2010;121:206-220.

20. Franc NC, Dimarcq J, Lagueux M, Hoffmann J, Ezekowitz R. Croquemort, a novel *Drosophila* hemocyte/macrophage receptor that recognizes apoptotic cells. *Immunity*. 1996;4(5):431-443.
21. Poon IKH, Lucas CD, Rossi AG, Ravichandran KS. Apoptotic cell clearance: basic biology and therapeutic potential. *Nature reviews. Immunology*. 2014;14(3):166-180. doi: 10.1038/nri3607.
22. Sheedy FJ, Grebe A, Rayner KJ, et al. CD36 coordinates NLRP3 inflammasome activation by facilitating intracellular nucleation of soluble ligands into particulate ligands in sterile inflammation. *Nature immunology*. 2013;14(8):812-820. doi: 10.1038/ni.2639.
23. Endemann G, Stanton L, Madden K, Bryant C, White R, Protter A. CD36 Is a Receptor for Oxidized Low Density Lipoprotein. *The Journal of Biological Chemistry*. 1993;268(16):11811-11816.
24. El Khoury JB, Moore KJ, Means TK, et al. CD36 Mediates the Innate Host Response to  $\beta$ -Amyloid. *The Journal of experimental medicine*. 2003;197(12):1657-1666. doi: 10.1084/jem.20021546.
25. Ockenhouse C, Tandon N, Jamieson G, Greenwalt D. Antigenic and functional differences in adhesion of *Plasmodium falciparum*-infected erythrocytes to human and bovine CD36. *Infection and Immunity*. 1993;61(5):2229-2232.
26. Triantafilou M, Gamper FGJ, Haston RM, et al. Membrane Sorting of Toll-like Receptor (TLR)-2/6 and TLR2/1 Heterodimers at the Cell Surface Determines Heterotypic Associations

with CD36 and Intracellular Targeting. *The Journal of biological chemistry*.

2006;281(41):31002-31011. doi: 10.1074/jbc.m602794200.

27. Hoebe K, Georgel P, Rutschmann S, et al. CD36 is a sensor of diacylglycerides. *Nature (London)*. 2005;433(7025):523-527. doi: 10.1038/nature03253.

28. Miao WM, Vasile E, Lane WS, Lawler J. CD36 associates with CD9 and integrins on human blood platelets. *Blood*. 2001;97(6):1689-1696. doi: 10.1182/blood.V97.6.1689.

29. Abumrad NA, Perkins RC, Park JH, Park CR. Mechanism of long chain fatty acid permeation in the isolated adipocyte. *The Journal of biological chemistry*. 1981;256(17):9183.

30. Abumrad N, Park J, Park C. Permeation of long-chain fatty acid into adipocytes. Kinetics, specificity, and evidence for involvement of a membrane protein. *Journal of Biological Chemistry*. 1984;259(14):8945.

31. Baillie AG, Coburn CT, Abumrad NA. Reversible Binding of Long-chain Fatty Acids to Purified FAT, the Adipose CD36 Homolog. *The Journal of membrane biology*. 1996;153(1):75-81. doi: 10.1007/s002329900111.

32. Febbraio M, Abumrad NA, Hajjar DP, et al. A Null Mutation in Murine CD36 Reveals an Important Role in Fatty Acid and Lipoprotein Metabolism. *The Journal of biological chemistry*. 1999;274(27):19055-19062. doi: 10.1074/jbc.274.27.19055.

33. Ibrahimi A, Bonen A, Blinn WD, et al. Muscle-specific Overexpression of FAT/CD36 Enhances Fatty Acid Oxidation by Contracting Muscle, Reduces Plasma Triglycerides and Fatty

- Acids, and Increases Plasma Glucose and Insulin. *The Journal of biological chemistry*. 1999;274(38):26761-26766. doi: 10.1074/jbc.274.38.26761.
34. Coburn CT, Knapp FF, Febbraio M, Beets AL, Silverstein RL, Abumrad NA. Defective Uptake and Utilization of Long Chain Fatty Acids in Muscle and Adipose Tissues of CD36 Knockout Mice. *The Journal of biological chemistry*. 2000;275(42):32523-32529. doi: 10.1074/jbc.m003826200.
35. Drover VA, Ajmal M, Nassir F, et al. CD36 deficiency impairs intestinal lipid secretion and clearance of chylomicrons from the blood. *The Journal of clinical investigation*. 2005;115(5):1290-1297. doi: 10.1172/JCI200521514.
36. Pownall H, Moore K. Commentary Fatty Acid Wars: The Diffusionists vs. the Translocatists. *Arteriosclerosis, thrombosis, and vascular biology*. 2014;34(5):e8-e9.
37. Xu S, Jay A, Brunaldi K, Huang N, Hamilton JA. CD36 Enhances Fatty Acid Uptake by Increasing the Rate of Intracellular Esterification but Not Transport across the Plasma Membrane. *Biochemistry*. 2013;52(41):7254-7261. doi: 10.1021/bi400914c.
38. Love-Gregory L, Sherva R, Sun L, et al. Variants in the CD36 gene associate with the metabolic syndrome and high-density lipoprotein cholesterol. *Human Molecular Genetics*. 2008;17(11):1695-1704. doi: 10.1093/hmg/ddn060.
39. Yamashita S, Hirano K, Kuwasako T, et al. Physiological and pathological roles of a multi-ligand receptor CD36 in atherogenesis; insights from CD36-deficient patients. *Mol Cell Biochem*. 2006;299:19-22. doi: 10.1007/s11010-005-9031-4.

40. Ma X, Bacci S, Mlynarski W, et al. A common haplotype at the CD36 locus is associated with high free fatty acid levels and increased cardiovascular risk in Caucasians. *Human molecular genetics*. 2004;13(19):2197-2205. doi: 10.1093/hmg/ddh233.
41. Putri M, Syamsunarno MRAA, Iso T, et al. CD36 is indispensable for thermogenesis under conditions of fasting and cold stress. *Biochemical and biophysical research communications*. 2015;457(4):520-525. doi: 10.1016/j.bbrc.2014.12.124.
42. Armesilla A, Vega M. Structural organization of the gene for human CD36 glycoprotein. *The Journal of Biological Chemistry*. 1994;269(29):18985-18991.
43. Silverstein RL, Febbraio M. CD36, a Scavenger Receptor Involved in Immunity, Metabolism, Angiogenesis, and Behavior. *Science signaling*. 2009;2(72):re3. doi: 10.1126/scisignal.272re3.
44. Febbraio M, Hajjar D, Silverstein R. CD36: a class B scavenger receptor involved in angiogenesis, atherosclerosis, inflammation, and lipid metabolism. *J Clin Invest*. 2001;108(6):785-791. doi: 10.1172/JCI14006.
45. Smyth M, Martin J. X Ray crystallography. *J Clin Pathol Mol Pathol*. 2000;53:8-134.
46. Alberts B, Johnson A, Lewis J. Analyzing Protein Structure and Function. In: *Molecular Biology of the Cell 4th Edition*. New York: Garland Science; 2002.

47. Neculai D, Schwake M, Ravichandran M, et al. Structure of LIMP-2 provides functional insights with implications for SR-BI and CD36. *Nature*. 2013;504(7478):172-176. doi: 10.1038/nature12684.
48. Gonzalez A, Valeiras M, Sidransky E, Tayebi N. Lysosomal integral membrane protein-2: A new player in lysosome-related pathology. *Molecular genetics and metabolism*. 2014;111(2):84-91. doi: 10.1016/j.ymgme.2013.12.005.
49. Hsieh F, Turner L, Bolla JR, Robinson CV, Lavstsen T, Higgins MK. The structural basis for CD36 binding by the malaria parasite. *Nature communications*. 2016;7(1):12837. doi: 10.1038/ncomms12837.
50. Wynn TA, Chawla A, Pollard JW. Origins and Hallmarks of Macrophages: Development, Homeostasis, and Disease. *Nature*. 2013;496(7446):445-455.
51. Varol C, Mildner A, Jung S. Macrophages: Development and Tissue Specialization. *Annual review of immunology*. 2015;33(1):643-675. doi: 10.1146/annurev-immunol-032414-112220.
52. Sica A, Mantovani A. Macrophage plasticity and polarization: in vivo veritas. *The Journal of clinical investigation*. 2012;122(3):787-795. doi: 10.1172/JCI59643.
53. Yao Y, Xu X, Jin L. Macrophage Polarization in Physiological and Pathological Pregnancy. *Frontiers in immunology*. 2019;10:792. doi: 10.3389/fimmu.2019.00792.
54. Orecchioni M, Ghosheh Y, Pramod AB, Ley K. Macrophage Polarization: Different Gene Signatures in M1(LPS+) vs. Classically and M2(LPS-) vs. Alternatively Activated Macrophages. *Frontiers in immunology*. 2019;10:1084. doi: 10.3389/fimmu.2019.01084.

55. Russell DG, Huang L, VanderVen BC. Immunometabolism at the interface between macrophages and pathogens. *Nature reviews. Immunology*. 2019;19(5):291-304. doi: 10.1038/s41577-019-0124-9.
56. Fraternali A, Brundu S, Magnani M. Polarization and Repolarization of Macrophages. *Journal of clinical & cellular immunology*. 2015;6(2). doi: 10.4172/2155-9899.1000319.
57. Woo M, Yang J, Beltran C, Cho S. Cell Surface CD36 Protein in Monocyte/Macrophage Contributes to Phagocytosis during the Resolution Phase of Ischemic Stroke in Mice. *The Journal of biological chemistry*. 2016;291(45):23654-23661. doi: 10.1074/jbc.M116.750018.
58. Pennathur S, Pasichnyk K, Bahrami NM, et al. The Macrophage Phagocytic Receptor CD36 Promotes Fibrogenic Pathways on Removal of Apoptotic Cells during Chronic Kidney Injury. *The American journal of pathology*. 2015;185(8):2232-2245. doi: 10.1016/j.ajpath.2015.04.016.
59. Raggi F, Pelassa S, Pierobon D, et al. Regulation of Human Macrophage M1–M2 Polarization Balance by Hypoxia and the Triggering Receptor Expressed on Myeloid Cells-1. *Frontiers in immunology*. 2017;8:1097. doi: 10.3389/fimmu.2017.01097.
60. Chen H, Li M, Sanchez E, et al. Increased Alternative Macrophage-2 (M2) Polarization with Trib1 Gene over Expression in Myeloma Patients with Progressive Disease and Jak2 Inhibitors Reduce M2 Polarization. *Blood*. 2015;126(23):1011. doi: 10.1182/blood.V126.23.1011.1011.
61. Marim FM, Silveira TN, Lima DS, Zamboni DS. A Method for Generation of Bone Marrow-Derived Macrophages from Cryopreserved Mouse Bone Marrow Cells. *PloS one*. 2010;5(12):e15263. doi: 10.1371/journal.pone.0015263.

62. Guthmann F, Haupt R, Looman AC, Spener F, Rustow B. Fatty acid translocase/CD36 mediates the uptake of palmitate by type II pneumocytes. *AJP - Lung Cellular and Molecular Physiology*. 1999;277(1):191-L196. doi: 10.1152/ajplung.1999.277.1.L191.
63. McCarty MF, DiNicolantonio JJ. Lauric acid-rich medium-chain triglycerides can substitute for other oils in cooking applications and may have limited pathogenicity. *Open Heart*. 2016;3(2):e000467. doi: 10.1136/openhrt-2016-000467.
64. Kar Niladri, Ashraf Mohammad, Valiyaveetil Manojkumar, Podrez Eugene. Mapping and Characterization of the Binding Site for Specific Oxidized Phospholipids and Oxidized Low Density Lipoprotein of Scavenger Receptor CD36. *Journal of Biological Chemistry*. 2008;283(13):8765-8771. doi: 10.1074/jbc.M709195200.
65. Pascual G, Avgustinova A, Mejetta S, et al. Targeting metastasis-initiating cells through the fatty acid receptor CD36. *Nature*. 2017;541:41-45.
66. Nilsen NJ, Deininger S, Nonstad U, et al. Cellular trafficking of lipoteichoic acid and Toll-like receptor 2 in relation to signaling; role of CD14 and CD36. *Journal of Leukocyte Biology*. 2008;84(1):280-291. doi: 10.1189/jlb.0907656.
67. Austyn J, Gordon S. F4/80, a Monoclonal Antibody Directed Specifically Against the Mouse Macrophage. *European Journal of Immunology*. 1981;11(10):805-815.
68. Jablonski KA, Amici SA, Webb LM, et al. Novel Markers to Delineate Murine M1 and M2 Macrophages. *PloS one*. 2015;10(12):e0145342. doi: 10.1371/journal.pone.0145342.

69. Hu JM, Liu K, Liu JH, et al. CD163 as a marker of M2 macrophage, contribute to predict aggressiveness and prognosis of Kazakh esophageal squamous cell carcinoma. *Oncotarget*. 2017;8(13):21526-21538. doi: 10.18632/oncotarget.15630.
70. Obesity and overweight. <https://www.who.int/news-room/fact-sheets/detail/obesity-and-overweight>. Accessed June 29, 2020.
71. Obesity in Canada – Health and economic implications. <https://www.canada.ca/en/public-health/services/health-promotion/healthy-living/obesity-canada/health-economic-implications.html>. Accessed June 29, 2020.
72. Puccetti L, Sawamura T, Pasqui AL, Pastorelli M, Auteri A, Bruni F. Atorvastatin reduces platelet-oxidized-LDL receptor expression in hypercholesterolaemic patients. *European Journal of Clinical Investigation*. 2005;35(1):47-51. doi: 10.1111/j.1365-2362.2005.01446.x.
73. Han J, Zhou X, Yokoyama T, Hajjar DP, Gotto AM, Jr, Nicholson AC. Pitavastatin Downregulates Expression of the Macrophage Type B Scavenger Receptor, CD36. *Circulation*. 2004;109(6):790-796. doi: 10.1161/01.CIR.0000112576.40815.13.
74. Krzyszczyk P, Schloss R, Palmer A, Berthiaume F. The Role of Macrophages in Acute and Chronic Wound Healing and Interventions to Promote Pro-wound Healing Phenotypes. *Frontiers in physiology*. 2018;9:419. doi: 10.3389/fphys.2018.00419/full.